MINISTRY OF EDUCATION AND RESEARCH
University POLITEHNICA of Bucharest
Doctoral School of
Industrial Engineering and Robotics

Ing. Tudor George D. ALEXANDRU

DOCTORAL THESIS

PhD supervisor,
Prof.dr.ing. Cristina PUPĂZĂ (UPB)

- 2021 -

MINISTRY OF EDUCATION AND RESEARCH
University POLITEHNICA of Bucharest
Doctoral School of
Industrial Engineering and Robotics

Ing. Tudor George D. ALEXANDRU

DOCTORAL THESIS

Machine learning generalization of the embedded systems cooling workflows for facilitating the smart retrofitting of computer control units employed in industrial engineering environments

SUMMARY

PhD supervisor,
Prof.dr.ing. Cristina PUPĂZĂ (UPB)

- 2021 -

UNIVERSITATEA POLITEHNICA DIN BUCUREȘTI
UPB
1818

University POLITEHNICA of Bucharest

Decision CSUD UPB no. ……. from ……………………

Tudor George D. ALEXANDRU

DOCTORAL THESIS

Machine learning generalization of the embedded systems cooling workflows for facilitating the smart retrofitting of computer control units employed in industrial engineering environments/

Generalizarea algoritmilor de învăţare automată pentru fluxurile de răcire ale sistemelor înglobate din unităţile de comandă-control utilizate în ingineria industrială pentru facilitarea procesului de modernizare inteligentă

DOCTORAL COMITEE

Committee Chairperson	Prof.dr.ing. Irina SEVERIN	University POLITEHNICA of Bucharest, Romania
PhD Supervisor	Prof.dr.ing. Cristina PUPĂZĂ	
Member	Prof.dr.ing. Athanasios MIHAILIDIS	Aristotle University of Thessaloniki, Greece
Member	Prof.dr.ing. Roland Iosif MORARU	University of Petroșani Romania
Member	Prof.dr.ing. Cătălin Gheorghe AMZA	University POLITEHNICA of Bucharest, Romania

- 2021 -

Contents

Preface

The cooling of embedded systems represents a limiting aspect in newly developed or retrofitted computer control units. Such devices stand at the core of any industrial engineering environment, acting as a binder between the physical motion of actuators and the computational intelligence of shop floor automation. The interdisciplinary aspects of thermal design and the knowledge required to tackle the underlying workflows of the process bring into discussion challenging engineering perspectives. My initial experience with electronics heat transfer occurred during my master's degree. During this time, I have gained valuable knowledge in computer aided engineering and experimental procedures. In this regard, I would like to express my gratitude to Professor Cristina Pupăză and Professor Adrian Florin Nicolescu for sharing their expertise in the two fields. Later on, I have won the first prize at a National Student Scientific Session hosted by the University of Petroșani in 2016. At the same time, I have co-authored two research papers in the field of electronics heat transfer. The ever increasing viewports of thermal design sparked my interest in developing a dissertation project related to this topic. My working experience as an aerospace stress engineer and the challenges of multiphysics simulations were the contributing factors for this decision. The literature survey that was carried out in the Master's thesis highlighted a significant literature gap of the subject in the context of Industry 4.0, in particular in the case of Smart retrofitting. My interest in the domain paved the way towards doctoral studies. In the first stage, I managed to develop a lumped parameter model for estimating power dissipation by combing the philosophies of structural design in aerospace engineering with my general knowledge of heat transfer. The findings of the research were disseminated in the International Conference on Electronics, Computers and Artificial Intelligence in 2019. I would like to address in this way my gratitude to Assystem Technologies Romania and the Aerospace Stress Engineering Team for sharing their knowledge and granting me access to the LMS Samtech solver. While the lumped parameter approach proved practical for standalone heat sources its applicability in case of multi-chip design was limited. In this regard, I have gained interest in studying Machine Learning algorithms, as a convenient way of generalizing experimental data. The findings of my research were disseminated at a seminar that was held at the University of Edinburgh – Artificial Intelligence and its Applications Institute in 2019. In this way, I would like to acknowledge the support of Professor Jacques Fleuriot for all his valuable comments and suggestions, which helped improve the quality of the work. The results were published in Studies in Informatics and Control – Q2 Journal in 2020. Another important aspect of cooling systems was identified as the temperature controller development process. In this regard, a finite element method PID controller was developed, including real-world considerations. Generalization of the controller outputs was achieved by employing recurrent neural networks. This topic is also of interest in my present career as Teaching Assistant at the Department of Robots and Manufacturing Systems, Faculty of Industrial Engineering and Robotics. In this regard, I appreciate the effort of Professor Tiberiu Dobrescu and Adrian Olaru for taking part in the scientific committee of research reports while providing me with the appropriate advice. I would also like to thank solid waste management expert Mihai Șolea for emphasizing the sustainability issues of the thermal design and for providing me the appropriate tools for benchmarking the carbon footprint of the process. A bonded heat sink was developed as an alternative way to lower the CO_2 emissions of thermal design. Alabandite was employed for manufacturing the cooling fins. This objective was achieved thanks to the collaboration with George Dincă, PhD. Researcher at the Geological Institute of Romania. Least but not last, I would like to thank my family for supporting me all this years, especially my sister for inspiring me with her enthusiasm and courage.

List of abbreviations

Nr. crt.	**Abrev.**	**Significance**
1	BC	Boundary Condition
2	CAE	Computer Aided Engineering
3	CPS	Cyber Physical Systems
4	CPU	Central Processing Unit
5	EOL	End-of-Life
6	FEM	Finite Element Method
7	LSTM	Long short-term memory
8	ML	Machine Learning
9	MpSoC	Multi core system on chip
10	PCB	Printed Circuit Board
11	PID	Proportional-Integral-Derivative
12	PWM	Pulse Width Modulation
13	ReLu	Rectified Linear Unit
14	RMSPror	Root Mean Square Propagation
15	RNN	Recurrent Neural Network
16	TC	Temperature gain of core i
17	TCP	Temperature gain of the entire package
18	TDP	Thermal Design Power
19	TTC	Time constant of core i
20	TTP	Time constant of the entire package

Section 1. Introduction

Industry 4.0 represents an ongoing improvement of products and product related services that aims the development of interconnected manufacturing systems [C02,D02]. Transformative and disruptive technologies have emerged in the past decades to support the industrial transformation process [B10]. In this regard, recently developed shop floor devices have an online identity, being able to exchange real-time information with the surrounding industrial ecosystems [Z01]. This process is carried out with the support of interrelated computing platforms (i.e. the Internet of Things or Cloud computing) [W01]. On the other hand, the decision taking tasks benefit from the extensive use of Machine Learning (ML) algorithms [R05, L12]. Cyber Physical Systems (CPS) stands at the core of Industry 4.0, being considered a synergy between mechatronics and real-time networking [P10]. The underlying hardware and software that is employed in the development of the aforesaid solutions is distinguished throughout the literature as Embedded System [D04, L07]. Such integrated circuits bring together computational elements, networking protocols and graphical user interfaces, acting as a binder between the decentralized shop floor intelligence and the physical motion of actuators [S02]. The ever increasing demand for virtual resources combined with the tight power and space constraints of autonomous devices bring into discussion challenging hardware perspectives [A02]. In this regard, the companies specialized in the development of embedded systems are continuously improving their product portfolio to meet the requirements of the Industry 4.0 market [L16]. Thus, the next generations of microcontrollers or small-configured computer control units incorporate a wide range of expansion ports, extended computational resources and data storage capabilities [S04]. Recently developed machine tools or shop floor devices benefit from such solutions, being considered Industry 4.0 ready [S08]. In major enterprises, the industrial transformation process gradually takes place by phasing out the obsolete computer control units and replacing them with CPS [S15]. In this way, stakeholders can fully take advantage of the cutting edge technologies of real-time networking [R03]. Even so, the costs and knowledge required to complete the process is less attractive to small and medium enterprises [M04]. In this regard, smart retrofitting has emerged as an alternative industrial transformation approach that aims upgrading the existing hardware or software of shop floor devices to meet the requirements of the Industry 4.0 platform [A13]. The process is carried out most of the times with the support of internal or external embedded systems that exchange information with the existing interfaces [L14]. From an economic point of view, smart retrofitting enables the development of CPS in emerging companies [G01]. Even so, the lack of process formalization and standardized product development procedures in the field brings into discussion custom tailoring workflows [G08]. This is due to the fact that not all computer control units are intended to facilitate future upgrades. Furthermore, each manufacturing system and shop floor device has its own operational requirements that might over constrain the upgrade process [C05]. As a consequence, the space, environmental and power domain of smart retrofitting projects is characterized by rigid boundaries. Such limitations can be addressed by dividing the problem into discrete disciplines, demanding specialized teams to deal with the underlying aspects of engineering knowledge (i.e. circuit diagram, microprocessor programming or device ergonomics). Nevertheless, the purpose of smart retrofitting is to facilitate the transition of existing automation towards Industry 4.0 by minimizing the resource requirements [D06]. In this regard, a wide range of software and tools have emerged to lower the complexity of the virtual prototyping stages (i.e. Computer Aided Design, Computer Aided Engineering or Electronic Design Automation) [M03]. On the other hand, high level application programming interfaces facilitate the development of real-time networking environments [S12]. Even so, a range of workflows are not fully covered by the existing software approaches. In particular, the cooling of embedded systems has become a limiting aspect of smart retrofitting [A11]. From a holistic point of view, this workflow encompasses two sub-workflows: thermal design and the development of temperature controllers. A brief description of the embedded systems cooling methodology is depicted in the continuing section.

1.1. Thermal design

Thermal design represents a branch of engineering design that deals with optimal component selection for developing cooling solutions for active heat sources found in electronic assemblies [G09]. A schematic representation of the process is depicted figure 1.1.

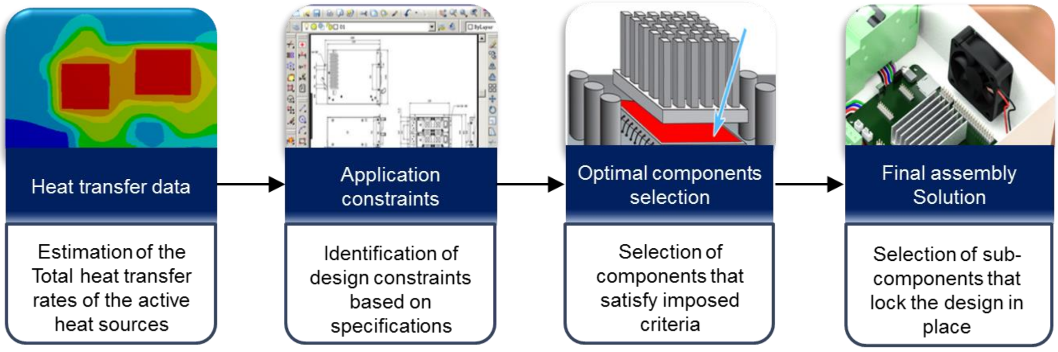

Fig. 1.1 A generalized thermal design framework

The methodology encompasses 4 distinct stages:

1. **The estimation of heat transfer data**: the semiconductors employed in the design of integrated circuits have the ability to opose the flow of electric current [J02]. The resulting energy is released at the main junctions of the package under the form of heat [L05]. Guidelines for estimating this quantity are depicted in the datasheets of any embedded heat source [D05]. On the other hand, a more precise definition of the power dissipation can be achieved by means of multiphysics simulation software [M02]. In this regard, engineers can capture the electromagnetic, electric, fluid and thermal domain of any heat source with the support of Computer Aided Engineering (CAE) software [J01]. Alternatively, experimental procedures can be employed to identify the temperature of the package under different operational scenarios [A15].
2. **Application constraints**: active or pasive cooling components (i.e. fans, heat sinks or blowers) are characterized by geometric specifications that are decided in accordance with the heat transfer data. In this regard, each embedded system has a limited amount of space for facilitating the implementation of such solutions. Therefore, engineers must carrefully examine the boundaries of the enclosure, the existing expansion capabilities and the inlet and outlet of the air guides. Additional constraints such as maximum allowed power for driving the cooling system must be taken into account.
3. **Optimal components selection**: based on the application constraints, a cooling solution comprising at least a heat sink is decided to exchange the heat generated by the integrated circuits with the surrounding environment [A06]. Forced convection devices are added most of the times to enhanche the thermal resistance of heat sinks, given the fact that the vast majority of embedded systems are air cooled [M09]
4. **Final assembly solution**: the catalogue specifications of the cooling components can only be satisfied in practice when the proposed solution is firmly mounted in place. In this regard, standardized brackets, assembly elements or custom tailored parts are

requiered to ensure an optimal thermal contact conductance between the heat exchanging elements [G07].

1.2. Temperature controllers

The instruction cycle of most embedded heat sources is characterized by a transient power dissipation processes that occurs mainly due to the resource usage [S14]. While thermal design solutions have the ability to maintain the temperature of the electronic components below their operation limits, the sudden increase or decrease of the temperatures at the main junction areas can have severe side effects on the life cycle of integrated circuits [S01]. Furthermore, operating cooling fans or blowers at 100% output at all times can prove ineffective when the resource usage is low or when the embedded system is found in an idle state [I03]. From this perspective, temperature controllers are employed as open or closed-loop feedback devices (Fig. 1.2) that maintain the temperature of heat sources at a desired value [A17].

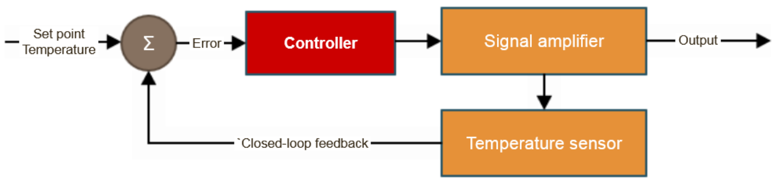

Fig. 1.2. A schematic representation of a generic closed-loop temperature controller

This objective is completed by acquiring information from temperature sensors throughout the instruction cycle of the system. The measured signal is compared to a set point value. The resulting error term is passed through a controller model. A process variable is generated at the output. An operational amplifier is deployed most of the times to convert this signal into a Pulse Width Modulated (PWM) one.

Based on the plant, two types of actuating signals can be generated:

1. **Adjustment of the cooling parameters**: represent most of the times PWM signals that dynamically adjust the behavior of the cooling fans or blowers. Thus, the convective heat transfer can be enhanced or reduced
2. **Adjustment of the resource usage**: the temperature of the heat source can be dynamically adjusted by varying its power dissipation. This scenario occurs in passive thermal design solutions. In such cases, the computational resources of the embedded systems can be decided in accordance with the temperature of the underlying electronic components.

Figure 1.3 depicts the stages of the controller development process:

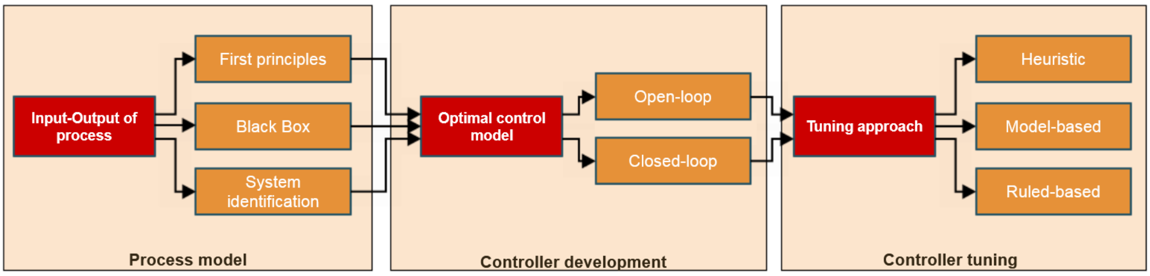

Fig. 1.3. The temperature controller development process

In the first stage, a process model is developed to describe the relationship between the input and the output of the physical system [S11]. In case of simple electronic components (i.e. resistors or diodes), the first principles approach is employed to derive a mathematical representation of the dynamic behavior of the heat transfer process [P04]. More complex embedded heat sources demand alternative procedures, such as the black box modeling technique [L01]. In this case, experimental studies are conducted to identify the transient response of the system without requiring explicit knowledge in its underlying heat transfer aspects. Alternatively, the system identification approach can be employed for the deriving process models based on statistical methods [S13].

In the next stage, the optimal controller is decided by taking into account the requirements and behavior of the system. In this regard, open loop control strategies can be used in case of heating elements or thermostats [S10]. On the other hand, the disturbances that occur in embedded systems demand most of the times closed-loop feedback. The most popular example in this case is the proportional-integral-derivative (PID) temperature controller [M13]. Other examples include the fuzzy logic or adaptive controllers [S19].

In the last stage, the parameters of the controller are decided in order to achieve a more robust or aggressive feedback strategy. For this purpose, heuristic tuning methods are employed when the initial value of the controller gains are known or can be estimated [J03]. Rule-based methods are used when the relationship between the control parameters and the response of the process model can be derived by mathematical models [P01]. On the other hand, model-based tuning can be carried out by evaluating the relationship between the control and output parameters of the system on physical hardware.

Section 2. The limiting aspects of existing approaches

The smart retrofitting process brings into discussion emerging thermal issues. This is due to the design constraints applied, the requirements of power saving in case of battery powered devices as well as the coexistence of multiple networking interfaces (Fig. 1.4):

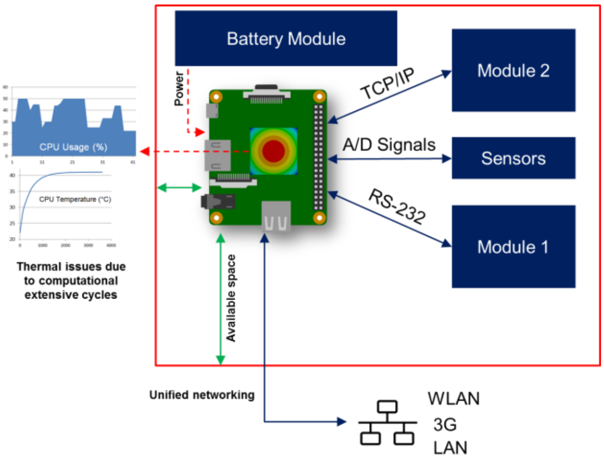

Fig. 1.4. Emerging thermal issues in smart retrofitting

A detailed description of these issues is discussed below:

- **Tight space constraints:** when performing smart retrofitting, the space available for deploying internal or external embedded systems is limited, considering that not all computer control systems employed in industrial engineering environments are intended for future upgrades. From this point of view, the adopted cooling solution is required to exhibit maximum efficiency in minimized space.
- **Power constraints:** the proliferation of battery powered devices (such as autonomous robots) demands extended efforts for minimizing the power draw such that the

operational range of the device can be increased. Therefore, a tradeoff is required between the cooling system efficiency and the power demanded by the active fans or blowers.

- **Extended computational demands:** intelligent systems and other transformative technologies demand a wide range of computational elements. Therefore, the amount of power released by the embedded heat sources is proportional with the resource usage.
- **Various interfaces:** Industry 4.0 relies on universal information exchange capabilities. This demands a wide range of hardware interfaces as part of CPS. Networking, signal processing or data transfer protocols result in additional hardware modules that represent sources of extra heat dissipation.
- **Unpredictable obsolescence:** Industry 4.0 is at the market acceptance stage. The ongoing development of embedded systems and software for smart devices results in the unpredictable obsolescence of previously implemented solutions. From this point of view, thermal design should be addressed with the focus on product re-use and appropriate end-of-life strategies.
- **Emerging environmental constraints:** Most thermal design solutions demand an increased amount of high thermal conductivity raw materials (i.e. aluminum or copper). The technologies required to manufacture heat sinks result in a high carbon footprint. While Eco-design solutions are adopted by major companies as part of the product development life cycle [K02], environmental engineering approaches for smart retrofitting are not well documented.

The smart retrofitting process applies additional constraints on the embedded systems cooling development workflow. In this regard, a practical study comprising an embedded Central Processing Unit (CPU) is provided to emphasize the influence of such limiting aspects on the thermal design and controller development stages.

1.3. Limiting aspects of the thermal design process

A Micro FC-BGA Case Intel CPU is subjected to a thermal design process. This type of package is widespread in the numeric control units of machining centers. The objective of the study is to adopt a forced convection heat sink that can satisfy the thermal resistance requirements of the package. According to the datasheet of the product, the studied CPU has the following thermal characteristics [I02]:

Table 1.2: Thermal design information for FC-BGA Intel Pentium III Class CPU

	Parameter	Value
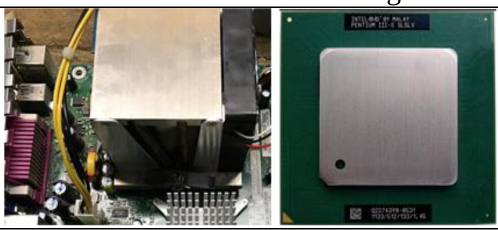	Allowable Junction Temperature (T_j)	100°C
	Thermal Design Power (P_{max})	16.12 W
	Allowable Ambient Temperature ($T_{Max\text{-}Ambient}$)	50°C

An analytical model is provided in [L08] for sizing a vertical plate heat sink under forced convection. For this purpose, Prandtl number (Pr) is defined, together with the expansion coefficient of the air β, determined as a constant for the optimum heat transfer rate dissipated from the fins for a given profile area.

In case of the present study, the proposed solution has a profile width of 30 mm, a fin thickness of 1 mm and a total mass of 77 g of Aluminum.

In practice, the thermal design power provided by the manufacturer represents the worst case scenario that is derived by employing laboratory testing standards. Such operating conditions rarely occur during in the life cycle of embedded systems.

An experimental assessment was carried out for the afromentioned setup. The results achieved indicate that the maximum power dissipation that occurs at 100% resource usage is evaluated at 9.85W, which is about 40% lower than compared to data sheet values.

The previous design was trimmed by adjusting the fins width. ANSYS Workbench steady-state thermal analysis was employed for developing this study [M10]. The new ambient temperature and convection coefficients due to geometry update are considered. Results indicate that an 11% saving of mass and space can be performed by adequately evaluating the behavior of the active heat source (Fig. 1.5 – a and b).

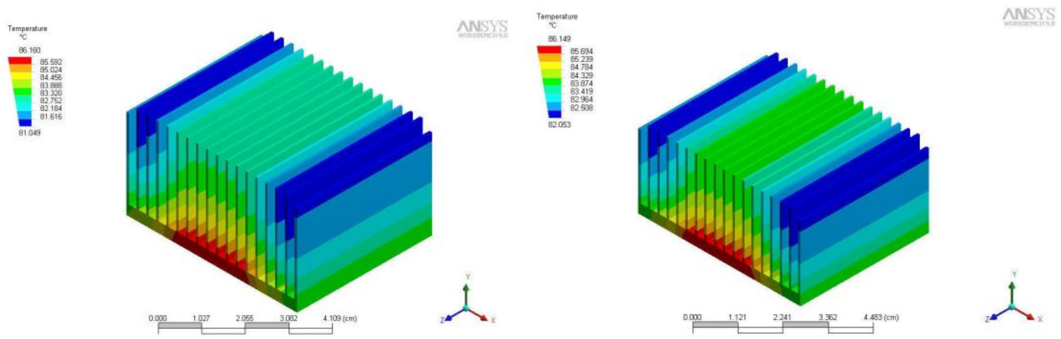

(a) (b)

Fig. 1.5. Space and material reduction study (a) baseline simulation (b) simulation based on experimentally assessed heat transfer rates

The results of the study emphasize the significant impact of employing conservative approaches for evaluating the power dissipation of embedded heat sources. On the other hand, achieving highly accurate results demands experimental procedures which are characterized by extended resource and time requirements. Furthermore, the procedure can only be conducted on physically available hardware.

1.4. Limiting aspects of the temperature controller development process

A temperature controller is developed with no explicit control engineering knowledge by employing MATLAB Simulink and System Identification toolboxes [S18]. The aim of the controller is to adjust the resource usage of the CPU (as the actuating signal) such that a set point temperature of 28°C is achieved. For this purpose, the relationship between the input and output signals of the open-loop process is modeled by means of a Laplace domain transfer function. In this regard, the CPU that was previously analyzed is subjected to a step signal that corresponds with the 100% resource usage. The relationship between the input and output variables is measured by experimental means (Fig. 1.6).

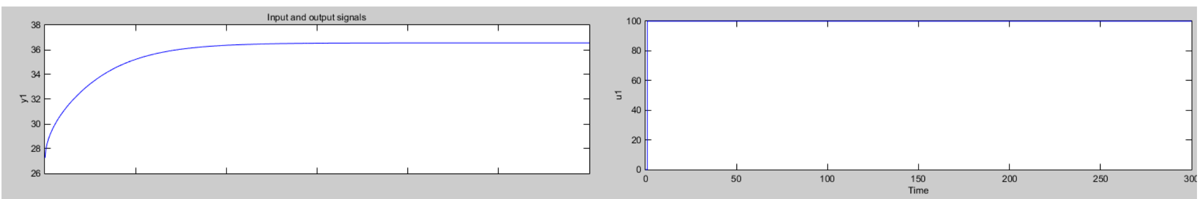

Fig. 1.6. The input-output relationship of the model

The system identification procedure is used to derive a 2 pole, one zero transfer function (the standard settings of the program). The resulting input-output model is translated to the Simulink environment for developing a PID temperature controller. Figure 1.7 depicts the schematic representation of the simulation model.

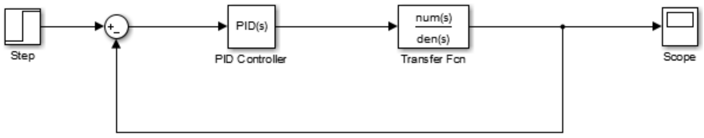

Fig. 1.7. Schematic representation of the Simulink model comprising a step signal, transfer function and closed-loop feedback PID controller

Tuning of the controller gains is completed by using the model-based method that is embedded in the Simulink Control design PID tuning tools. This procedure interactively identifies the gains with respects to the response of the system. A step-signal is employed at the input of the model to verify the behavior of the controller.

In the next stage, the process variable of the controller is exported for scheduling the resource usage of the CPU in the real-world environment. A comparison is performed between the experimental and simulation temperature curves (Fig. 1.8)

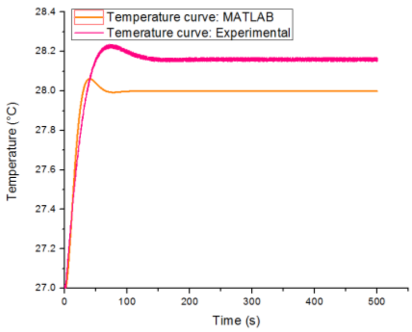

Fig. 1.8 The input-output relationship of the model

Table 1.3 depicts the main characteristics of the simulated and real-world signals:

Table 1.3 The performance and robustness of the simulated and real-world controller.

Characteristic	**Simulated signal**	**Real-world signal**
Rise-time	19 seconds	34.5 seconds
Settling time	55.2 seconds	111 seconds
Overshoot	7.19%	5.77%

The results achieved indicate different robustness and performances characteristics between the real-world vs. simulated controllers. This is due to certain aspects of control engineering that are neglected by the system identification approach. In this regard, the process dead time or the delay between the input and output signals is not taken into account [H06]. Furthermore, the simulated controller can adjust the amplitude of the actuating signal between infinite bounds. On the other hand, the limitations of the physical hardware, such as the saturation limits are not considered [B09]. As a consequence, the temperature controller development process can only be addressed with reasonable control engineering knowledge as well as adequate software and experimental tools.

Section 3. Conclusions

Smart retrofitting represents an alternative industrial transformation approach that aims upgrading the obsolete computer control units of shop floor devices. In this way, conventional automation can be converted into CPS with the support of additional hardware platforms. This process benefits from a wide variety of computer aided software as well as high level application programming interfaces. Even so, a limited range of workflows bring into discussion custom tailoring issues given the peculiarities of each computer control unit and the surrounding industrial ecosystem. In this regard, the cooling of embedded systems represents a limiting aspect of the smart retrofitting projects. This is due to the emerging space, power and environmental constraints. The present chapter performs a breakdown of the underlying disciplines of the process. A practical example is provided to emphasize the literature gap of embedded systems cooling in the present industrial context.

The following research objectives can be suggested:

1. **The development of an adequate methodology for addressing the power dissipation of embedded heat sources:** both thermal design and control engineering disciplines demand an appropriate description of the thermal behavior of integrated circuits. From this perspective, conservative approaches can prove a low level of accuracy while multiphysics simulation procedures demand extended resources, being less attractive in case of smart retrofitting projects.
2. **The generalization of the temperature controller development process:** numeric computing environments provide the necessary toolboxes for developing temperature controllers. Even so, the successful implementation of such concepts demands adequate control engineering knowledge. In this regard, the generalization of existing simulation, tuning and implementation procedures must be carried out to facilitate the development of temperature controllers in smart retrofitting.
3. **The analysis of sustainability aspects:** cooling components and their operation are a source of carbon footprint throughout the life cycle of embedded systems. In case of smart retrofitting, the frequent upgrades of computer control units can cause environmental side effects. This is mainly due to the fact that the vast majority of heat sinks employ non-ferrous materials. Such issues must be taken into account to ensure a sustainable product development policy in smart retrofitting.

The three research topics represent the objectives of the present Doctoral Thesis. In this regard, the continuing chapters provide methodologies for dealing with the aforementioned issues as follows:

- **Chapter 2:** provides a lumped parameter approach for estimating the power dissipation of standalone electronic components. The methodology is based on the theoretical aspects of first order systems. Experimental methods and the total heat transfer rate thermal networks are employed for supporting the process.
- **Chapter 3:** the lumped parameter approach developed in section 2 provides a low level of flexibility due to its high reliance on experimental data. Machine learning regression is employed to overcome such issue. Furthermore, the given concepts are extended to meet the requirements of electronic components comprising multiple heat sources in the same package.
- **Chapter 4:** addresses the limiting aspects of the temperature controller development process by proposing a PID temperature controller that is based on finite element method (FEM) thermal analysis. Generalization of the procedure is achieved by including the real-world considerations of convective heat transfer and actuator saturation. The implementation of the controller in a real-world environment is carried out by employing a Recurrent Neural Network (RNN) that can predict the relationship between the input and output variables for any given operational scenario.
- **Chapter 5:** the environmental issues of the heat sink manufacturing technologies are addressed by means of a sustainable product development approach. The methodology investigates the integration of alabandite as an alternative material for the design of cooling fins in forced convection environments. Comparative studies are conducted to evaluate the achievable carbon footprint savings.

Section 1. The Lumped parameter approach

2.1. General aspects

A brief overview of the information presented in the previous chapter reveals the need to support the embedded systems thermal design process with accurate heat transfer rates. In accordance with the recent trends in the field, such approaches facilitate space and resource savings [F01, A10]. Even so, the complexity of the existing methodologies brings into discussion time, knowledge and economic constraints. Therefore, the underlying design and simulation procedures are only attractive to embedded systems developers, rather than industrial end users. From this perspective, effective upgrade or retrofitting options rely on fast and accurate solutions.

Lumped parameter models represent an alternative to the existing heat transfer estimation methods [W03, R01]. The methodology involves the use of discrete entities that divide the thermal domain into constitutive blocks. Each block describes the interaction between the physics involved (Fig. 2.1).

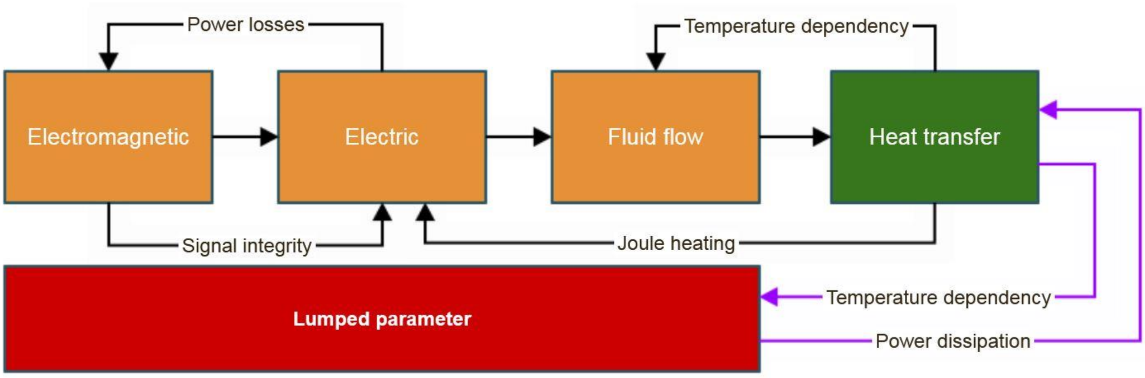

Fig. 2.1 Discrete entities for Lumped parameter method

In this way, the electromagnetic, electric and fluid flow domains are encompassed in time or temperature dependent characteristics that can be evaluated by means of experiments [W08]. Thus, the multiphysics viewports of the problem can be captured by indirect variables.

2.2. Theoretical considerations

The heat transfer in electronic components can easily be described by means of the thermal network model (Fig. 2.2) [A16].

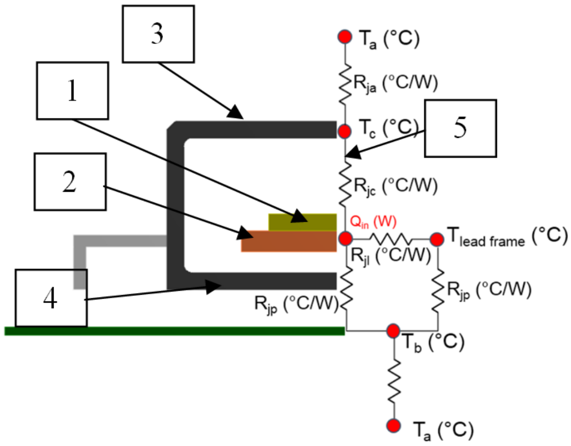

Fig. 2.2. Equivalent thermal network of an active heat source

The chip (1) that is attached to the die (2), transfers the heat by conduction (for solid material filled case) or radiation (for electronic components filled with protective gases) to the case (3). Two main junctions can be distinguished [S09]:

- The junction between the Case and the Printed Circuit Board (PCB) (4)
- The junction between the Case and the ambient or a cooling solution (5)

From a steady-state point of view, each junction is characterized by a thermal resistance (R); representing the difference between the temperatures at two nodes (n_i) divided by the heat flow occurring due to the electrical resistance of the chip (Q_{in}) [S07]:

$$R = \frac{T_{n_i} - T_{n_i+1}}{Q_{in}} \tag{2.1}$$

From a transient point of view, the ability of the electronic package to store and remove heat is characterized by the thermal capacitance (C), defined as the ratio of change in heat stored (kcal) and change in temperature (°C). By considering the mass of the electronic die (M – kg) and the specific heat of the bonding material (C_p - Kcal/Kg°C), the thermal capacitance can be described as [H03]:

$$C = M \cdot C_p \tag{2.2}$$

Based on equations 2.1 and 2.2, the relationship between the input (R) and output (S) of a simple linear thermal system resembles a first order differential equation under the form [B07]:

$$\frac{C(s)}{R(s)} = \frac{K}{T \cdot S + 1} \tag{2.3}$$

Where K is the gain and T the time constant of the system.

Equation 2.3 can be employed to approximate the dynamic behavior of thermal systems with a reasonable degree of accuracy [M11]. Even so, the stack-up of non-linear materials that coexist in the design of embedded electronic components limit the practical use of first order systems transfer functions, demanding the use of more complex input-output models.

A study is conducted in this regard by considering a RAM module that is subjected to a maximum usage step response. The test platform is depicted in figure 2.3.

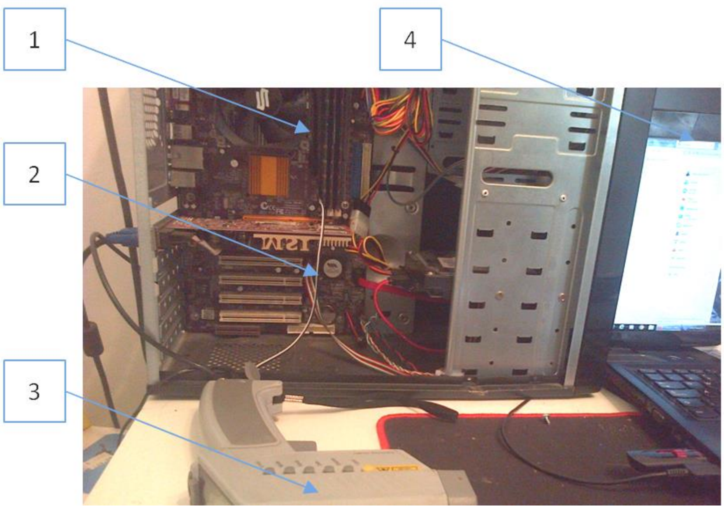

Fig.2.3. The test platform

A DDR memory package (1) operates at a frequency of 400 MHz with a supply voltage of 2.6V. An Omega TC-PVC-K24-180 high fidelity thermocouple is glued at the case-to-ambient junction surface of one of the memory chips (2). The serial interface of an infrared pyrometer (3) is used for data acquisition. MATLAB software is employed to store the time vs. temperature curves on a portable PC (4). At full load, the power dissipated by the each memory bank is 5.408W. The test conditions comprise two stages: idle – 1 second; 72 seconds – 100% fill with zeros.

Based on equation 2.3 and the relationship between the input and the output of the thermal system, the transfer function of the model can be written in Laplace transformation form as:

$$\frac{C(s)}{R(s)} = \frac{28.55}{6s+1} \tag{2.4}$$

The denominator in equation 2.4 represents a static gain of 28.55°C that is derived by subtracting the maximum temperature of the memory module from the ambient one. On the other hand, the time constant of the first order function is 6 seconds, representing how quickly the system reacts to a change in its input.

The zero state response of the studied system (zs) can be written as:

$$C_{zs}(s) = H(s) \cdot R(s) = \frac{K}{T \cdot S + 1} \cdot \left(\frac{1}{s}\right) = \frac{28.55}{s \cdot (6s+1)} \tag{2.5}$$

The Inverse Laplace transformation of equation 2.5 is carried out in equation 2.6:

$$L^{-1} = \frac{571}{20} - \frac{571 \cdot e^{-\frac{t}{6}}}{20} \tag{2.6}$$

Figure 2.4 –a depicts the graph of equation 2.6 in comparison with the zero-state of the real-world system under step input (the ambient temperature of 22°C is taken into account) while figure 2.4 – b emphasizes the behavior of the system when a square input is applied.

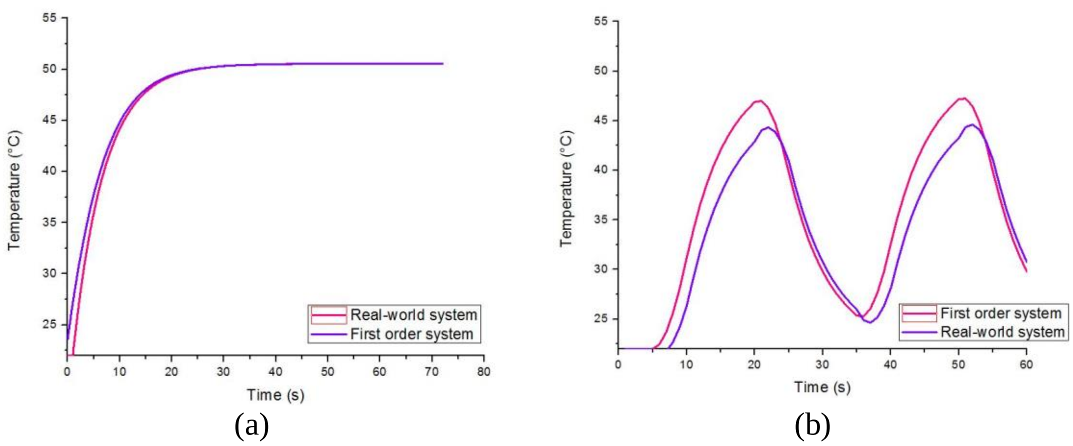

Fig. 2.4. Step response of the first order transfer function vs. real-world system

The output of the first order transfer function model is less accurate when the input is a transient one. The error between the results depicted in figure 2.4 can be explained by the non-linear behavior of the materials that are embedded in the chip, die and lead-frame of the heat source [L13, L11].

By considering the non-linear behavior of embedded heat sources, the use of first order systems to approximate their behavior can only provide a coarse description of the underlying heat transfer mechanism.

One approach for tackling such issues is to divide the system into discrete states that are materialized by first order characteristic curves. For the example provided, 5 states can be distinguished corresponding with the 20-40°C ambient temperature ranges. Each state has its own temperature gain and time constants (Table 2.1).

Table 2.1. Experimentally derived gains

Ambient temperature (°C)	**Gain (°C)**	**Time constant**	**Transfer function**
20	24.72	7.11	$\frac{24.72}{7.11s+1}$
25	24.95	7.11	$\frac{24.95}{7.11s+1}$
30	25.19	7.04	$\frac{25.19}{7.04s+1}$
35	25.42	7.04	$\frac{25.42}{7.04s+1}$
40	25.66	7.04	$\frac{25.66}{7.04s+1}$

The differences between the transfer functions of each operational state emphasizes the ability of modeling the non-linear heat transfer behavior of embedded electronics by means of first-order systems with variable gains and time constants, in accordance with the operating temperature of the package. An algorithm is proposed for embedding the given concepts in a programming language:

Algorithm for variable transfer function

Procedure lumped (substeps, t, tf, K, T_s, T, signal, state)
- **for** each substeps **do**
  - **if** t = 0 then output = tf (K,T_s) for signal (t=0) + T_0
    - **else**
    - K,Ts = state (t=i)
    - output = tf (K,Ts) for signal (t=i) + T_{i-1}
  - **end if**

end procedure

The lumped procedure is carried out for a specific time domain that is divided into a number of substeps that have a constant or variable step size (t). For each substep an input signal (signal) is passed through a first order transfer function (tf) that is characterized by a gain (K) and a time constant (T_s). An initial state is considered when t=0. Afterwards, the temperature increase of the electronic package determines the present and future state in which the system operates (state) and subsequently the underlying K and T_s values.

2.3. Software implementation

FEM heat transfer analysis represents a first order system that is governed by equation 2.7 [P12]:

$$[C]\{\dot{T}\}+[K]\{T\}=\{Q^a\} \tag{2.7}$$

Where: C represents the specific heat matrix, K the conductivity matrix, T the vector of nodal temperatures and Q^a the applied heat flow vector. The procedure for solving equation 2.7 is the generalized trapezoidal rule [S20]:

$$\{T_{n+1}\} = \{T_n\} + (1-\theta)\Delta t\{\dot{T}_n\} + \theta\Delta t\{\dot{T}_{n+1}\} \tag{2.8}$$

Where: θ represents a transient integration parameter, $\Delta t = t_{n+1} - t_n$, T_n the nodal temperature at a given time step. Because most transient thermal simulations are non-linear, the Newton-Raphson procedure is deployed for solving the resulting equations [B05].

An analogy is performed between the theoretical model and the simulation one:

- **First order system**: replaced by 2D / 3D membrane elements subjected to power dissipation and conductive and/or convective heat transfer
- **Variable gain**: temperature dependent conductance imposed by 1D conductive link elements
- **Variable time constant**: temperature dependent capacitance modeled by means of 0D thermal mass elements

2.4. Assumptions made

The practical use of the element is presented in figure 2.5.

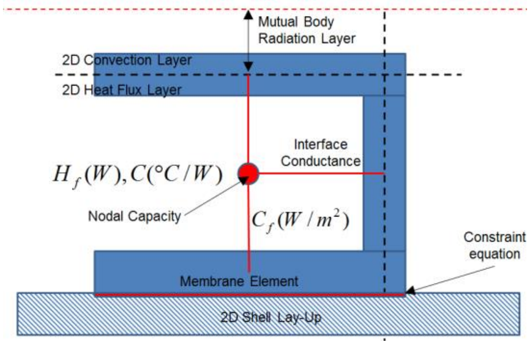

Fig. 2.5 Representation of the lumped parameter simulation model

The illustrated setup comprises an electronic circuit that is embedded in a rectangular case. Thin shell surfaces are employed to model the exterior boundaries of the package. These membrane elements have negligible thickness and thus negligible capacitance. Furthermore, each surface has independent nodes that are not coupled one to another at the boundaries [H04]:

$$T = \frac{1}{2}\left[T_i\left(-s+s^2\right) + T_j\left(s+s^2\right) + T_k\left(1-s^2\right)\right] \tag{2.9}$$

Where: T represents the temperature DOF of the element; i, j, and k are the constitutive nodes and s the heat flow vector. No thermal gradients occur as a consequence of the element's topology and shape function.

The power dissipation location is materialized by a centroid node. Interface conductance bars are deployed to transfer the heat to the negative side of the membrane elements [B01]:

$$q = k_x \cdot \frac{(T_i - T_j)}{L} \tag{2.10}$$

Where: q represents the thermal flux, k_x the conductivity and L the distance between the i and j nodes. Each element is linked with the surrounding elements by using nodal coupling constraints.

Capacitance of the electronic component is modeled with the support of a 0D nodal capacity element, positioned at the same coordinates as the central node [G04]:

$$\left[C_e^t\right]=\left[C_a\right] \tag{2.11}$$

Where: C_e^t represents the specific heat and C_a the capacitance matrices. This element is used to model a body with no significant thermal gradients, allowing the transient equilibrium condition to be achieved with a single parameter – the body capacitance (J/°C).

In total, the lumped parameter model comprises 6 thin shells with 4 independent nodes and 6 interface conductance bars that share a common node in the centroid of the box. The other end of the bars is linked with the adjacent nodes of the shells with the support of constraint equations.

Based on Fourier's law of conduction, a temperature gradient occurs between the interior and exterior walls of the electronic package. The cold surface is materialized by a 2D convection layer. Mutual body radiation occurs between the heat source and an exterior surface of the enclosure. The interaction between the membrane elements and a PCB is modeled with the support of constraint equations.

Parameterization of conductance and capacitance is carried out by means of experimental data. The strategy is to analyze the operational states (described in the previous section) of the heat source by using a single experimental procedure.

Section 2. Verification of the given concepts

To prove the given concepts, a study is carried out regarding the thermal behavior of a Socket 478 Intel Pentium IV Processor. Being widespread in industrial robot controllers, this CPU will be tested by considering two different platforms and instruction cycles. The thermal network of the package is captured by using an AsRock P4I65g motherboard. The experimental layout is emphasized in Fig. 2.6.

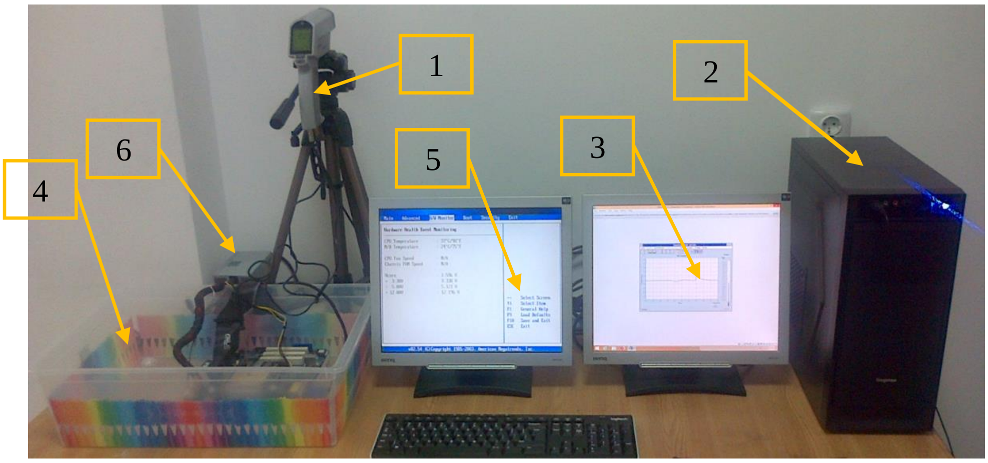

Fig. 2.6 The Experimental test platform

A Raynger MX infrared pyrometer equipped with a TC-K Thermocouple (1) is connected to a PC (2) by means of an analogue connection. Data acquisition is completed by using the pyrometer's proprietary software (3). A plastic tray (4) is deployed to ensure the optimal position of the mainboard-CPU assembly, such that the external thermal influences are limited. The VGA output of the mainboard is connected to an external display (5). The motherboard's power supply and data storage unit (6) are positioned outside the tray. A custom built heat sink is deployed having a hole drilled at the center. A TC-K thermocouple is attached to the CPU's thermal interface. To avoid the over heating of the processor, an axial fan is mounted on the left side of the heat sink, that is powered by an external power source in order to achieve a constant airflow. An embedded version of Microsoft Windows operating system was installed. All power management technologies were shutdown. No drivers were initialized and most of the operating system services were disabled. In this way, the additional resource usage is minimized. A software procedure is employed to apply a constant load on the CPU. 100 operational states are tested ranging from 1 to 100% usage.

Figure 2.7 depicts the experimentally derived results for different operational states (40 to 60% resource usage).

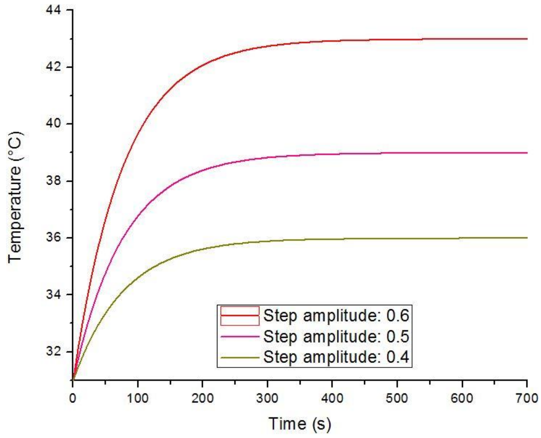

Fig.2.7. Experimentally derived operational states of the CPU

The experimental results are used to parameterize conductance and capacitance in the simulation model.

In the next stage, the CAE approach is completed in ANSYS Workbench 16.2 by using the integrated SAMCEF Interface for Steady State and Transient thermal simulations.

The accuracy of the approach is verified by considering a transient instruction cycle. For both comparison and verification purposes, figure 2.8 illustrates two plots side by side: (a) represents the results achieved by simulation and (b) represent the results achieved by experimental assessment.

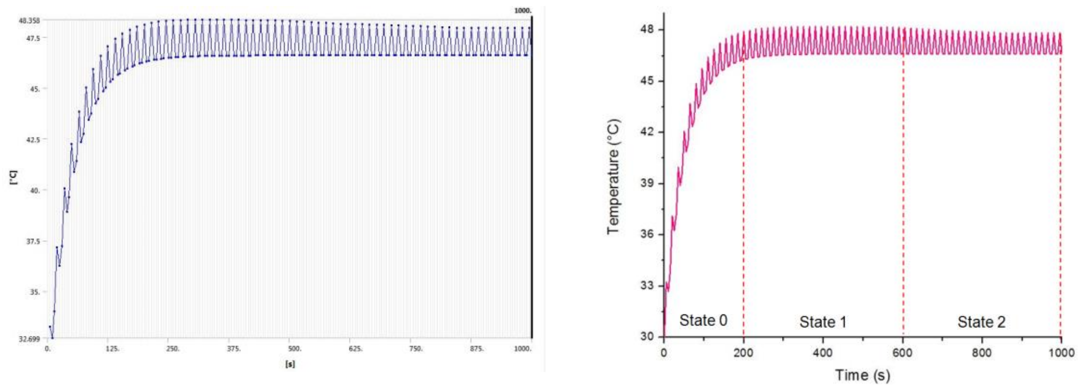

(a) (b)

Fig. 2.8 Time vs. temperature plot for a transient cycle – (a) experimental assessment and (b) simulation model

Simulations vs. experimental errors are evaluated in table 2.2 for the first maximum temperature occurrence point.

Table 2.2 Results and error percentage

Simulation Results		**Experimental results**		**Errors**	
Maximum Temperature (°C)	**At time increment (s)**	**Maximum Temperature (°C)**	**At time increment (s)**	**For Maximum Temperature (%)**	**For Time increment (%)**
48.358	205	48.15	200	0.43%	2.5%

The results achieved prove the practical use of the lumped parameter model for evaluating the total heat transfer rate in embedded systems. The knowledge captured can successfully be re-used for similar heat sources as long as the test platform employs comparable soldering technologies.

Section 3. Conclusions

The total heat transfer rate evaluation process represents an essential stage of any thermal design process. While conservative approaches exist, their use in smart retrofitting is limited given the tight space and power constraints. To overcome such issues, the present chapter proposes a lumped parameter approach that is based on the theoretical considerations of first order systems. The given concepts are transposed to a FEM simulation environment with the support of variable conductance and capacitance macro elements. The parameterization of the thermal analysis is achieved by means of experimental data. Experiments are conducted throughout the work to prove the practical use of the approach for evaluating the thermal behavior of standalone heat sources. The methodology can successfully be re-used when the package was previously studied. Alternatively, a coarse description of the total heat transfer rate can be achieved by extrapolating the results for new electronic components.

The original contributions of the work can be grouped in the following categories:

1. **Theoretical contributions**: the use of first order systems with adjustable temperature gain and time constants for developing a lumped parameter input-output model.
2. **Methodological contributions**: the development of experimental procedures for system identification purposes and the further use of the results for parameterizing transient thermal analysis
3. **FEM Modeling original contributions**: the practical use of a macro element for lumped parameter modeling based on temperature dependent conductance and capacitance
4. **CAE implementation:** A SAMCEF-ANSYS original implementation was completed.
5. **Experimental procedure:** the development of an original temperature acquisition procedure and processing of the results.

The results of the present chapter focused solely on standalone heat sources such as single core CPUs. Considering the proliferation of multi core system on a chip (MpSoC) solutions as part of high performance Industry 4.0 oriented embedded systems, the given concepts can be extended by adding sets of nodes - interface conductance elements for each independent core. In this case, a study of each individual heat source is required. This leads to a significant increase in the number of experimental assessments, making the approach less attractive. Machine learning software can be deployed to lower the dependency on experimental data whilst ensuring a good quality of the results by means of data analytics solutions. These topics will be addressed in Chapter 3.

The findings of the research were published in:

- **Alexandru, T. G.**, Mantea, T. A., Pupaza, C., & Velicu, S. (2016). Heat transfer simulation for thermal management of electronic components. Proceedings in Manufacturing Systems, 11(1), 15.
- **Alexandru, T.G.** & Pupaza, C. (2019), "An approach for estimating the total heat transfer rates in embedded systems", The 11th International Conference of Electronics, Computers and Artificial Intelligence (ECAI), pp. 1-6, 2019, WOS: 000461147400095

Section 1. Standalone heat source generalization

3.1. General aspects

In Smart Retrofitting the selection of the optimal embedded systems for upgrading the computer control units of shop floor devices is carried out prior to the purchase of the physical hardware [A14]. Hence, the adequate evaluation of the total heat transfer rate of the underlying electronic components must rely on the existing knowledge that is gathered by the company from similar projects [A05]. As a consequence, the thermal behavior of integrated circuits can only be recreated with a coarse level of detail. In this regard, a more effective knowledge capture approach consists of using computer algorithms for identifying the regularities in the given data [Z02]. In this way, the inputs of the lumped parameter model can be further used for generalizing the output variables with the support of regression algorithms [P02]. ML regression has long been a convenient way of dealing with non-linear data [K01]. Two approaches are the most common ones: the linear regression and the neural network models [G03]. The diversity of heat sources deployed in embedded systems, combined with the thermal behavior of each electronic package demands extended datasets for training, testing and generalization purposes. Traditional ML algorithms have a low performance when dealing with large datasets [T01]. Such aspects become even more limiting when the input data has noise [S03]. To overcome such issues, deep learning algorithms have emerged as a subset of ML [B04]. Such supervised learning models can deal with large datasets comprising noisy data. The prediction performance is proportional to the amount of data that is fed in [T03]. A typical deep learning regression model comprises a neural network that has multiple hidden layers of fully connected neurons [E01]. The strength of the connection is materialized by a weight [D08]. Non-linearity is added with the support of an activation function [S06]. The ability of the model to generalize unseen data relies on the optimizer employed for minimizing the cost function [L06]. This process is carried out by dynamically updating the weights during the training process (Fig.3.1).

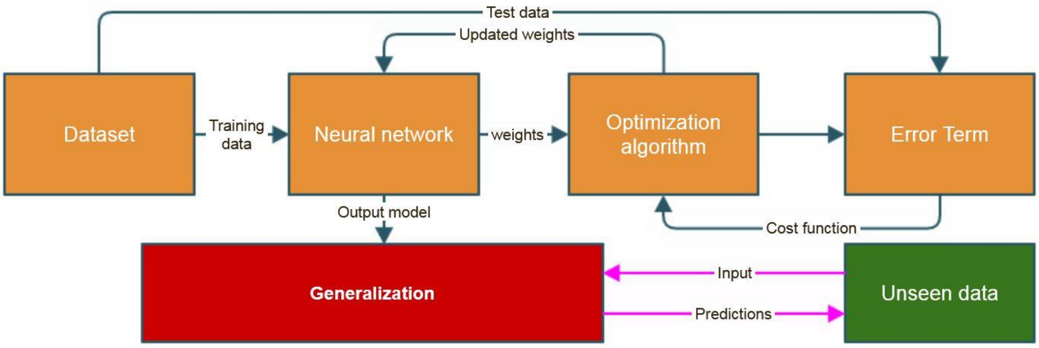

Fig. 3.1 The general structure of a deep learning regression model

3.2. Theoretical considerations

ML regression represents a set of statistical methods that are widespread in economic and industrial fields to determine the relationship between one dependent variable (the label) and a single or multiple independent variables (the features) [M01]. In the present study, the input data of the problem comprises characteristics that are in a close relationship with the thermal behavior of an electronic package (i.e. the supply voltage, operating frequency or die size) while the output corresponds with the variables required for the definition of the lumped parameter model (the temperature gain and time constants). The most popular ML technique for predicting continuous variables is the linear regression method. For a dataset comprising a single feature column (s), the regression label (p) is an explicit function such that [W06]:

$$p = f(s) \tag{3.1}$$

A family of rules is defined to express the link between the features:

$$f(s) = a \cdot s + b \tag{3.2}$$

With a and b being the unspecified parameters (or degrees of freedom) that are defined based on the available data. The target of the linear regression analysis is to identify the optimal values for a and b such that the squared error sum between the true and predicted output is minimized [S16].

In case of multiple inputs, the problem becomes a multiple linear regression one [M07]:

$$f(s_1, s_2) = w_{11} \cdot s_1 + w_{12} \cdot s_2 \tag{3.3}$$

Where: w_{11} and w_{12} represent weights.

An experimental study is carried out to prove the practical use and limitations of simple linear regression models. For this purpose, an ARM single board computer is subjected to a RGBenchMM floating point operations benchmark procedure [M12]. This device was deployed in an industrial engineering environment for monitoring the noise level of shop floor devices. A variable speed cooling fan is deployed to ensure the reliable operation of the device (Fig. 3.2)

.

Fig.3.2. ARM based single board computer with custom tailored cooling system

The objective of the study is to record the thermal behavior of the CPU (as label) by varying the temperature in the enclosure and the input voltage of the fan (as features). A dataset is developed comprising the results for 1000 test conditions. The dataset is divided 80% for training and 20% for testing the prediction accuracy. TensorFlow with Keras ML library for Python is used to develop the linear regression model and minimize the cost function. The gradient descent optimization method is employed for deciding the optimal weights. The objective is to minimize the root squared error cost function (J) by computing its gradients with respect to the parameter θ for the entire dataset [R06].

$$\theta = \theta - \eta \cdot \nabla_\theta \cdot J(\theta) \tag{3.4}$$

The Keras layer normalization is employed to bring the input variables to the same range (between 0 and 1).

The generalization ability of the model is low given the non-linear relationship between the independent (the voltage and the internal temperature) and dependent variable (the CPU temperature). As a consequence, linear regression analysis proves to be of limited use in the estimation of heat transfer characteristics (Fig.3.3).

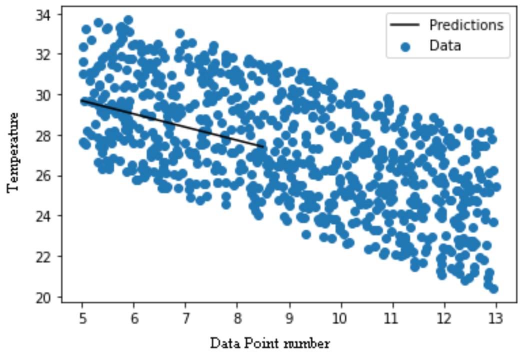

Fig.3.3. Multiple linear regresion prediction accuracy

To overcome such issues, a feed forward neural network is deployed instead. Such models define a set of points in space and the regression target is to identify the optimal ones with respect to a chosen metric. This metric is defined as the error term that penalizes instances of the model that are too complex or too far from the target [W07].

For the example provided, a ML learning regression model comprising two inputs (the voltage of the fan – i_1 and the temperature inside the enclosure – i_2) and one output (the temperature of the CPU – o) can be developed by means of multiple linear regression. To address the non-linearity of the model, an activation function (a) is added to equation 3.5 [K05]:

$$f_2(i_1, i_2) = a \cdot (w_{11} \cdot i_1 + w_{12} \cdot i_2) \tag{3.5}$$

In this case, the model is no longer characterized by a single output but rather by intermediate features of the function n, called l. For the example provided, 3 such features are considered:

$$\begin{aligned} l_1 &= a \cdot (w_{11} \cdot i_1 + w_{12} \cdot i_2) \\ l_2 &= a \cdot (w_{21} \cdot i_1 + w_{22} \cdot i_2) \\ l_3 &= a \cdot (w_{31} \cdot i_1 + w_{32} \cdot i_2) \end{aligned} \tag{3.6}$$

The final output of the model is calculated as:

$$\begin{aligned} f_3(v,t) &= a \cdot (v_1 \cdot l_1 + v_2 \cdot l_2 + v_3 \cdot l_3) = \\ &= a \cdot [v_1 \cdot a \cdot (w_{11} \cdot i_1 + w_{12} \cdot i_2) + v_2 \cdot a \cdot (w_{21} \cdot i_1 + w_{22} \cdot i_2) + v_3 \cdot a \cdot (w_{31} \cdot i_1 + w_{32} \cdot i_2)] \end{aligned} \tag{3.7}$$

Where: v and w represent weights.

Equations 3.5 to 3.7 describe the mathematical representation of a feed forward neural network comprising 2 input neurons (i_1 and i_2), one hidden layer (materialized by 3 neurons) and one output neuron (corresponding with the regression target – o). The graphical representation of the neural model is depicted in figure 3.4.

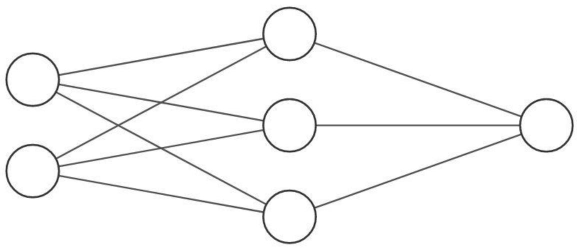

Fig.3.4. Architecture of the feed forward neural network

The new architecture is implemented in TensorFlow by replacing the previous linear regression one. The Rectified Linear Unit (ReLu) activation function is used for the hidden layers. The function returns 0 for any negative input and the input value for any positive x [C01]:

$$f(x) = \max(0, x) \tag{3.8}$$

A summary of the parameters employed for the training process is presented below:

- Feed forward Neural Network;
- Features were normalized;
- One hidden layer with 3 neurons was defined;
- Rectified Linear Unit (ReLu) activation function is used for the hidden layers;
- The gradient descent optimizer is employed to adjust the weights such that cost function is minimized;
- A learning rate of 0.01 is defined to control the weights with respect to the gradient loss;
- The Mean Squared error loss functions is used as model convergence metrics (typical to a regression problem);
- 100 Epochs are carried out (the dataset is fed to the algorithm backward and forward and batches are divided in 100 samples);

After each epoch, the cost function of the model is minimized (Fig. 3.5).

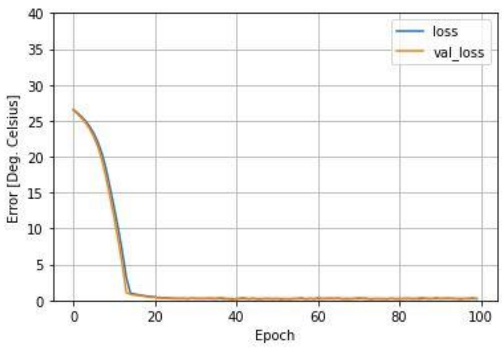

Fig.3.5. The minization of the cost function after 100 epochs

The mean absolute error derived by the program at the end of the training process is 0.254°C.

Opposed to the linear regression model, the feed forward neural network has the ability to learn the general features of the model. Furthermore, the optimization process converges to a model instance that does not capture undesired noise proving good generalization abilities by avoiding overfitting.

3.3. The deep learning regression model

Regression analysis based on feed forward neural networks proves a good ability to learn the general features from a dataset. Even so, the use of such models for embedded electronic components can prove challenging due to the increased number of features required for developing the dataset, as well as the non-linearity that governs the dynamics of the heat transfer process.

Deep learning has evolved as a broader family of ML that aims modeling data with a high level of abstraction [O01]. A deep learning regression model comprises a neural network with multiple hidden layers. In this way, the primitive features of the data are distinguished from the high level ones [L04]. Thus, the non-linear patterns of the input can be correlated with the output. Figure 3.6 depicts the structure of a deep network for regression analysis:

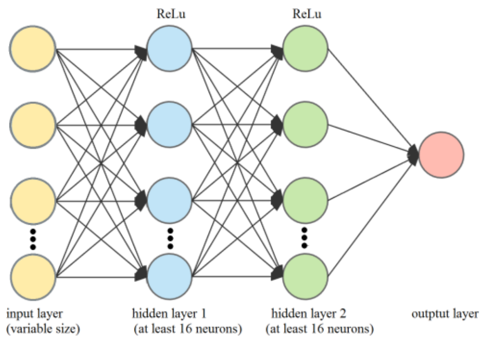

Fig.3.6. General structure of a deep network for solving regression problems involving embedded heat sources

3.3.1. The definition of the dataset

A dataset is developed comprising a wide range of single core CPUs. The selection includes a variety product families, models and performance specifications. The following hardware platforms are considered:

The features that are found in a close relationship with the temperature gain and settling time of the CPUs under various operational states are decided as: the socket, FSB (MHz), wattage (or thermal design power - W), Frequency (MHz), L2 cache (Kb), the number of transistors and the core voltage (V core – V). These features are extracted from the product specification manual of each CPU.

The labels are derived by employing the same experimental procedure depicted in Chapter 2 section 2.3. Figure 3.7 depicts an example of time constants (a) and temperature gains (b) for the AMD Athlon64 3000+ CPU.

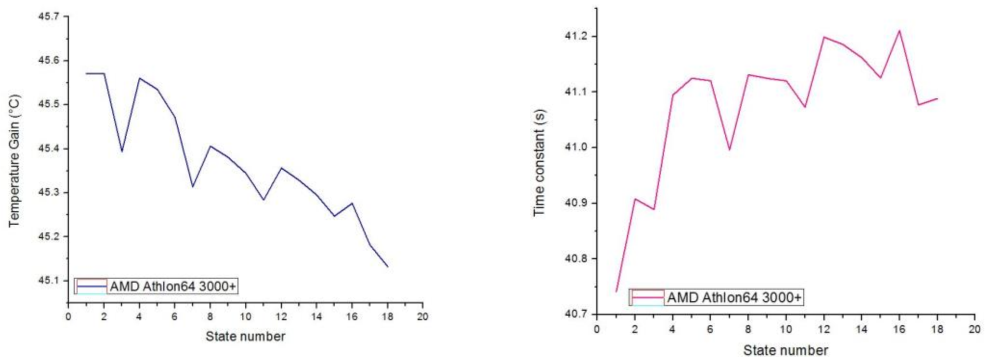

(a) *(b)*

Fig.3.7. Experimentally derived temperature gain – (a) and Time constant – (b) for the AMD Athlon64 3000+ CPU

3.3.2. The parameters of the deep network

The parameters that proved the best generalization ability for embedded heat sources under various operational states can be summarized as:

- Deep Neural Network;
- Normalized features;
- Two hidden layers;
- Each hidden layer has at least 16 neurons;
- Dataset was split 80% for training and 20% for testing the prediction accuracy of the model
- Rectified Linear Unit (ReLu) activation function is used for the hidden layers;
- Root Mean Square Propagation (RMSProp) optimization is employed to adjust the weights;

- A learning rate of 0.01 is defined;
- The Mean Squared error loss function is decided as model convergence metrics;
- 100 Epochs are carried out (the dataset is fed to the algorithm backward and forward and batches are divided in 100 samples);

3.3.3. The convergence of the model

The cost function of the model is minimized after 100 epochs, the mean absolute error being 1.05°C (Fig.3.8).

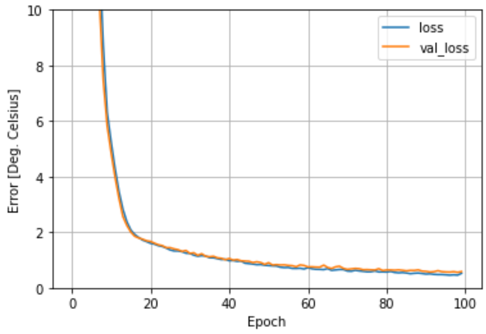

Fig.3.8. The minization of the cost function after 100 epochs

Section 2. Extension to multiple heat sources

The proposed approach focuses on the estimation of the total heat transfer rate for heat sources found in embedded systems, in particular, multi-core processors or multi-processor system-on-a-chip devices. To develop a lumped parameter approach applicable to such problems, it is imperative to capture all underlying physics by a reduced number of variables [A09]. The methodology can be divided in 3 layers (experimental, machine learning and simulation layer). The relationship between them is depicted in figure 3.9.

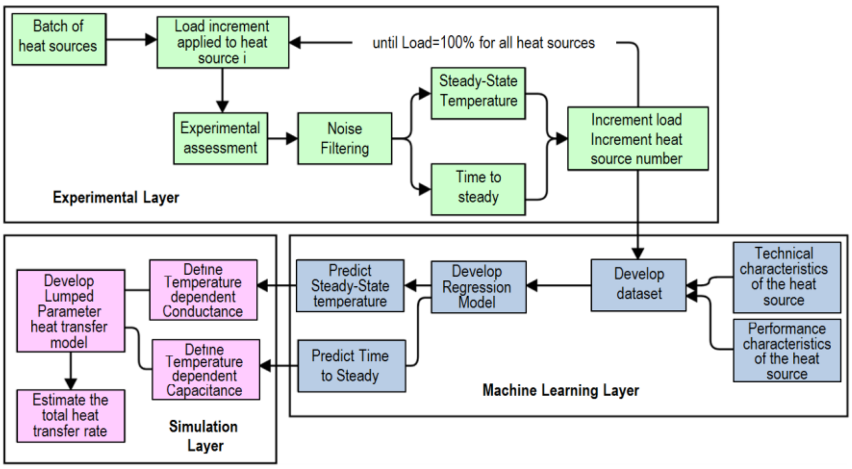

Fig.3.9. A schematic representation of the proposed approach for multi-chip modules

Each constitutive block of the proposed approach is detailed in the sections below:

3.4. The experimental layer

A batch of CPU samples was decided by considering their technical and performance specifications. The aim of the study is to have a consistent number of specimens that can cover a wide range of manufacturers (AMD, Intel and VIA), number of cores (dual, triple and quad core), frequencies (MHz), thermal design power specifications - TDP (W), lithography technologies (Nm), die sizes (mm2) and performance benchmark scores.

The experimental setup is identical to the one depicted in Chapter 2 - Section 2. An automated procedure is developed to adjust the amplitude of the step signal and to change the affinity of the CPU. In this way, the temperature gain and time constants are evaluated for all cores and combination of cores. All measurements are assembled in a single CSV file. Labels are added at the beginning and end of each experimental sequence for delimiting the acquisition cycles.

3.5. The ML layer

For the present study, a dataset is developed comprising features that are extracted from the technical and performance specifications of the studied CPUs. Thermal behavior data is included from the experimental layer. Categorical features are converted to numerical ones. A sample dual core CPUs dataset is presented in figure 3.10.

Thermal Specifications						Load Data				Experimental Data					
						Load Applied to		Step amplitude		Temperature gain (°C)			Settling time(s)		
Manufacturer	Frequency (MHz)	TDP (W)	Litography (Nm)	CPU Mark Score	Die Size (mm^2)	LC1	LC2	LPC1	LPC2	TC1	TC2	TCP	TTC1	TTC2	TTP
1	3000	65	45	1741	117.5	1	0	10	0	26.802	27.139	24.578	59.414	58.940	60.788
1	3000	65	45	1741	117.5	0	1	0	10	26.168	25.652	24.943	63.063	62.016	63.786
1	3000	65	45	1741	117.5	1	1	5	5	27.156	26.579	25.269	63.989	64.532	65.072

Features | Labels

Fig.3.10.The feature columns of a dataset applicable to dual core processors

The first 6 columns include the datasheet and performance specifications of the studied CPUs. Column 7 and 8 represent a load matrix. When 1 is applied on LC1 and 0 on LC2 that means that the load will be applied only on the second core. Column 9 and 10 materialize the step amplitude. For example, when LPC1 is set to 10% and LC1 is set to 1, LC2 to 0 that means that 10% resource usage is applied on core 2. Columns 11 to 16 indicate the temperature gain and settling time for the given operational state for each core (TC and TTC) and for the entire CPU package (TCP and TTP).

3.6. The simulation layer

The proposed simulation approach consists of a hollow structure comprising 2D skin elements of negligible thickness. The full details of the CPU case exterior are considered in the geometric model. Inside the case, each core is modeled by using a rectangular plate representation. Each element has a constant temperature, gradients being avoided by separating the boundary nodes. Thermal mass is taken into account for the individual cores and the entire CPU package. A graphical representation of the approach is depicted in figure 3.11.

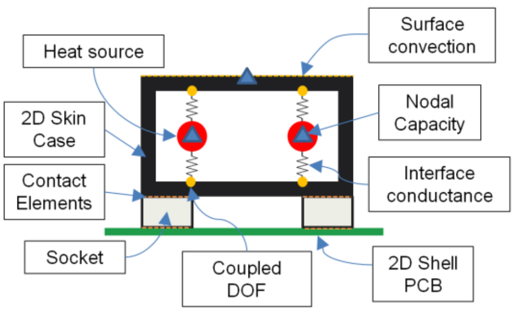

Fig.3.11 Graphical representation of the finite elements comprising the simulation layer

3.7. Case study

A case study regarding the smart retrofitting of a computer control unit from an industrial robot controller is performed (Fig. 3.12).

Fig.3.12. Main computer unit of an ABB IRC5 controller subjected to smart retrofitting

The aim of the upgrade is to replace the obsolete motherboard and CPU used in the original configuration with an embedded system that can draw less power while providing extended networking protocols and computational resources. The CPU used in the upgrade is a Dual Core AMD Athlon II X2 B24.

The dataset and the procedure of the regression analysis are depicted in Section 3.2.2. After 100 epochs, the training accuracy is ±2.02°C while the test set prediction accuracy is ±2.51°C. With the cost function minimized, the convergence of the model is optimal.

To prove the practical use of the approach a 5 second – full load, 5 second idle instruction cycle is defined in the simulation model. The resource usage acts on both of the CPU cores.

In the next stage, the results of the simulation model are verified by means of experiments. In this regard, the same instruction cycle is considered in the real-world setup. The experimental vs. simulation temperature curves are depicted in figure 3.13 for the case and cores.

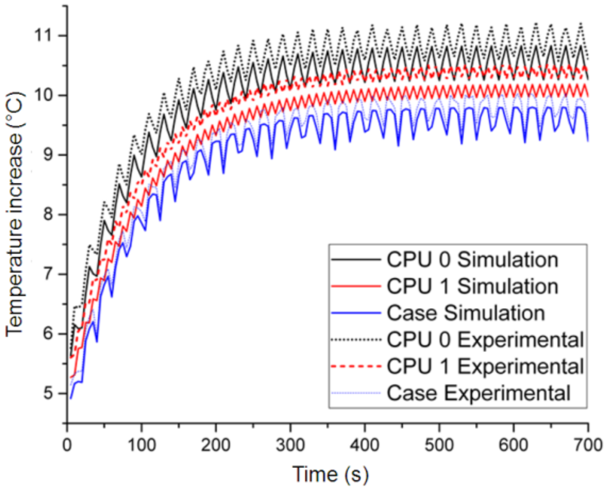

Fig.3.13 Comparison of experimental vs simulation values

A quick overview of the results achieved indicates the fact that the error between the experiments and simulations is a constant one. Even so, differences can be noticed between the slopes of the two temperature curves. This is due to various sources of error, including data acquisition, ML prediction errors and errors resulting due to the approximate methods used by the FEM solver.

Section 3. Conclusions

Describing the total heat transfer rate in multi-chip electronic components represents a challenging perspective due to the complexity of the underlying thermal networks. In this regard, the lumped parameter methodology developed in the previous chapter proves of limited use given the extended number of experimental variables required for parameterizing the model. Furthermore, the initial finite element model is only appropriate for studying each heat generating location at a time. To overcome such issues, the present chapter proposes the practical use of ML to predict the temperature gain and time constants based on the technical and performance specifications of the studied package. Changes are included in the initial simulation model to take into account the additional junctions.

The original contributions of the work can be grouped in the following categories:

1. **Theoretical contributions**: applied studies regarding machine learning regression analysis and the use of different learning architectures for the generalization of experimental data in single and multi-chip heat sources.
2. **Methodological contributions**: the development of a Visual Basic application tool for the automated parameterizing of lumped parameter models based on experimental data (not included in the summary).
3. **FEM Modeling original contributions**: the extension of the original lumped parameter simulation model to include multiple thermal junctions.
4. **CAE implementation:** A SAMCEF-Patran original implementation was completed.
5. **Experimental procedure:** an original experimental platform and the post-process of the results.

The findings of the research were published in:

- **Alexandru, T.G.** & Pupaza, C. (2020), "Machine learning generalization of lumped parameter models for the optimal cooling of embedded systems", Studied in Informatics and Control, Vol.28, Iss.2, pp. 1-6, 2019: WOS: 000573723600003, Impact factor 2019: 2.102 (**Q2**)
- **Alexandru, T.G.**, & Pupăză, C. (2021). Recurrent neural network for predicting time step bisections in structural dynamics, UPB. Scientific Bulletin, Vol. 83, Iss.1, pp.169-180.
- **Alexandru, T.G.** (2019, September). CISA Seminar - An approach for facilitating thermal design through the use of intelligent systems for Industry 4.0. Available at: https://www.edinburgh-robotics.org/events/cisa-seminar-approach-facilitating-thermal-design-through-use-intelligent-systems-industry-40, accessed: 25.09.2021

The generalized lumped parameter model has the ability to capture the thermal behavior of both standalone and multi-chip components. In this regard, engineers can adequately evaluate the power dissipation for achieving accurate thermal design solutions. From this perspective, the next objective consists in addressing the issues of the temperature controller development process in the next Chapter of the work.

Section 1. FEM PID temperature controllers

4.1. General aspects

The cooling of Embedded Systems represents an engineering design workflow that is deployed in newly developed or retrofitted computer control units [P08]. The aim of the process is to ensure the safe and reliable operation of the entire shop floor device by maintaining the temperature of its active electronic components (i.e. CPUs, memory modules or networking chips) under their operational limit [D10]. This objective is completed with the support of active (i.e. fans or blowers) or passive cooling components (i.e. heat sinks or fluid flow ducts) that operate in a closed-loop control environment [W04]. Figure 4.1 depicts an overview of the Embedded Systems cooling workflow stages.

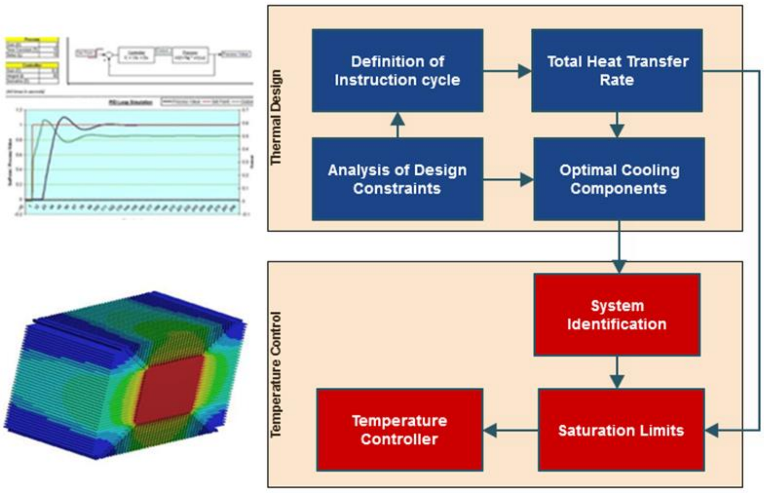

Fig.4.1 A holistic overview of the Embedded Systems cooling workflow stages

From a holistic point of view, the constitutive blocks of the process can be encompassed in two distinct sub-workflows: thermal design [G02] and the development of temperature controllers [H01].

4.2. Theoretical considerations

The development of FEM PID temperature controllers is carried out with the support of unidirectional elements. Such simulation procedures benefit from spring-damper-sliding capabilities, being widespread in FEM solvers for replicating the behavior of thermostats, relief valves or friction clutches [T06]. The typical structure of a unidirectional element deployed in a thermal system is depicted in figure 4.2.

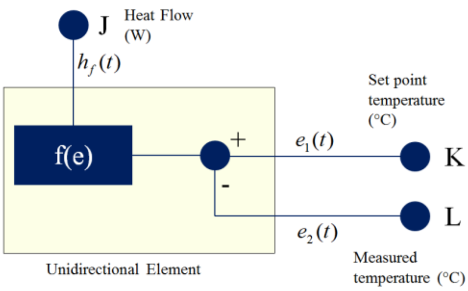

Fig. 4.2 Unidirectional element deployed in transient thermal analysis systems

Nodes K and L represent the control nodes. The set point value is applied as a boundary condition (BC) at node K. Node L is attached to a specific location in the model that corresponds to the temperature sensor. The element internally subtracts the temperature at Node K (e_1) from Node L (e_2). Moreover, it allows a mathematical operation on this resulting error term (e). The output of f(e) represents a heat flow acting on node J (h_f) that is proportional to (e):

$$h_f(t) = k_i \cdot |f(e)| \tag{4.1}$$

Where: k_i represents a constant gain.

The equations that are deployed in the case of the three elements are described below [M06]:

- Proportional controller:

$$h_f = e_1 - e_2 \tag{4.2}$$

- Integral controller

$$h_f = \int_0^t (e_1 - e_2)dt \tag{4.3}$$

- Derivative controller

$$h_f = \frac{d(e_1 - e_2)}{dt} \tag{4.4}$$

Section 2. The proposed approach

The formalization of the Embedded Systems cooling workflow involves two major objectives: the re-use of the engineering knowledge gained throughout the thermal design stages and the development of a unified simulation environment for tackling both sub-workflows. From this perspective, the proposed approach comprises 3 layers of abstraction.

The outcome of the approach is to develop a cooling fan speed scheduling procedure for direct use in an existing Embedded System. This is achieved by using the power dissipated by the heat source during the instruction cycle as simulation input. A ML procedure using a Long short-term (LSTM) recurrent neural network is proposed for tackling the issues related to the computational efficiency of the resulting controller model.

A schematic representation of the proposed approach is depicted in figure 4.3.

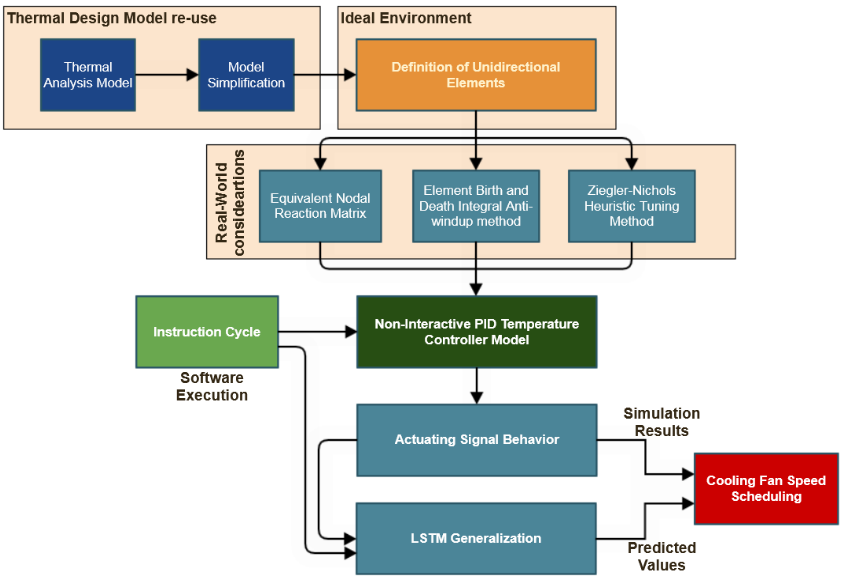

Fig.4.3 A schematic representation of the proposed approach

A detailed description of the main constitutive blocks is performed in the sections below.

4.3. Model simplification

A 2D simulation approach can be used to reduce the dimensional space of the model. The methodology is applicable to extruded heat-sinks that are subjected to thermal loads and BCs that act on the entire profile length. The size of the model can be further reduced by deploying symmetry BCs, allowing a quarter or half of the geometry to be analyzed when the applied heat flow is symmetric.

4.4. Definition of Unidirectional elements

Three unidirectional elements are required for implementing a PID controller as part of a transient thermal analysis. Figure 4.4 depicts a schematic representation of the proposed implementation strategy for a single fin heat sink that is subjected to a laminar air flow.

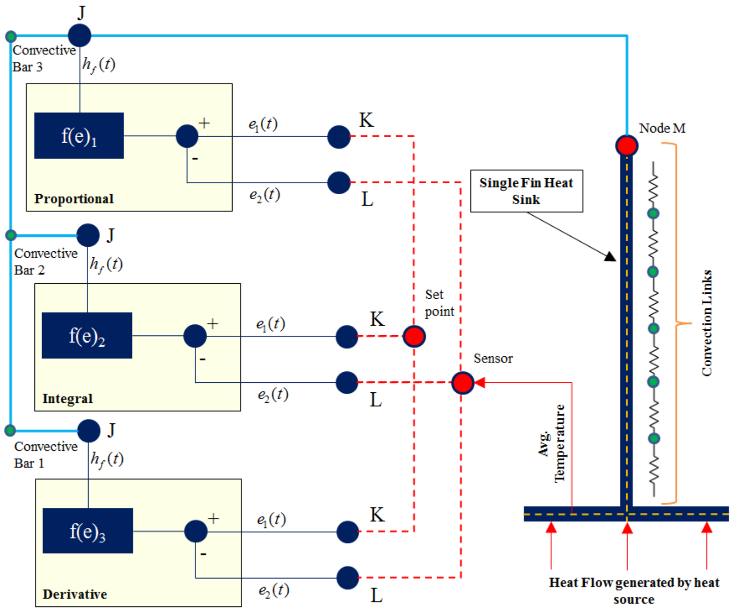

Fig.4.4 FEM PID Controller implementation strategy

For all unidirectional elements deployed, nodes K and L are coincident. The value that is measured at node L corresponds to the average temperature at the junction between the heat-sink and the heat source. 1D convective bars are deployed to link nodes J with node M which represents the tip of the fin. The heat flow rate equation is described as [***02]:

$$q = h_f \cdot A \cdot (T_i - T_j) \tag{4.7}$$

Where q represents the heat flow rate (W), h_f represents the film coefficient (W/m^2°C), A the area (m^2) and T the temperature at one of the element's nodes (°C).

In case of the conductive bars deployed for linking nodes J and M, an arbitrary large value is decided for h_f, the area of the element being equal to the edge area associated with node M. Thus, the resistance of the two nodes is matched.

Convective bars are deployed to enforce this behavior by linking all the vertical plane nodes with node M. For each connection, a specific value is defined for h_f. In this way, the resulting network of thermal resistors adjusts the energy removed from the system, similar to a convection BC.

Another important issue in the design of PID controllers is the dead time [D01]. This process delay represents the transportation lag between the input and output signals. In case of the FEM environment, the density and specific heat of the geometry account for this effect. Even so, additional delay occurs due to the frequency of the acquisition system [T04]. From this point of view, a 0D thermal mass element can be attached to the base of the heat sink nodes to take into account the additional package capacitance.

4.5. Equivalent Nodal Reaction Matrix

The FEM PID controller has the ability to remove energy from the system by replicating the behavior of a convection BC that acts on the vertical planes of the fin. Even so, this controlled variable does not correspond to any parameter of the physical process. From this point of view, an approach is required to convert the generated heat flow (W) into the rotational velocity of a cooling fan (RPM) or other meaningful quantities. A schematic representation of the proposed procedure is depicted in figure 4.5.

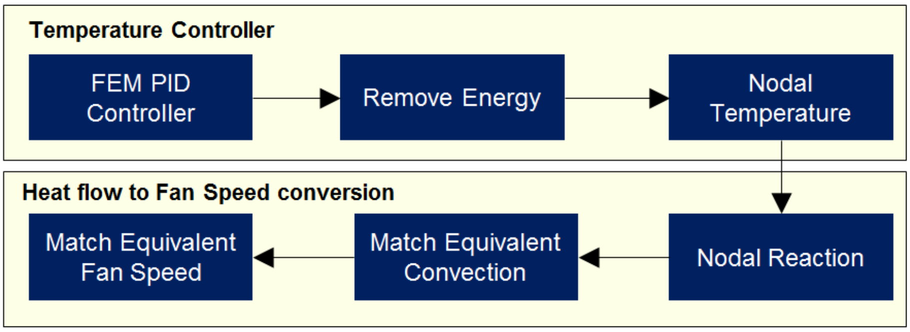

Fig. 4.5 A holistic overview of the Embedded Systems cooling workflow stages

In the first stage, a parametric study is developed to identify the relationship between the average vertical plane heat flow and an equivalent convection film coefficient (W/m^2°C). For this purpose, the power that is dissipated by the heat source during the instruction cycle of the Embedded System is used as input in the baseline simulation model. The coefficient of the vertical planes convection is set constant. The solver outputs the nodal reaction values for all of the nodes found in the location of the BC, for each time step of the simulation. In the next stage, the initial film coefficient is incremented. As a consequence, the temperature in the systems will decrease, resulting different nodal reactions. A matrix (M) is deployed to emphasize this behavior:

$$M = \begin{bmatrix} -2.1975E-7 & -4.3950E-7 & -6.5925E-7 & -8.7900E-7 \\ -6.2193E-7 & -1.2439E-6 & -1.85E-6 & ... \\ -1.0241E-6 & -2.0482E-6 & ... & ... \\ -1.8285E-6 & ... & ... & ... \end{bmatrix} \tag{4.9}$$

The matrix from equation 4.9 consists of 4 rows and 4 columns. Each row corresponds to the time step while the columns depict the value of the applied convection film coefficient. Each entity from the matrix represents the average nodal reaction occurring on the vertical planes of the fin.

4.6. Element Birth and Death Integral Anti-windup method

Actuators deployed in thermal design solutions are characterized by a saturation (or region of operation) limit. One issue in the proposed FEM controller is the linear behavior of the actuating signal. As a consequence, infinite heat flow can be generated to compensate the increase of the system temperature. The second issue that is also in a close relationship to saturation is the integral windup. This situation occurs when a large change in the set point takes place causing the integral term to accumulate error [K08]. As a consequence, the controller overshoots as the error is unwound [T05]. The clamping method is deployed to tackle both issues (Fig. 4.6).

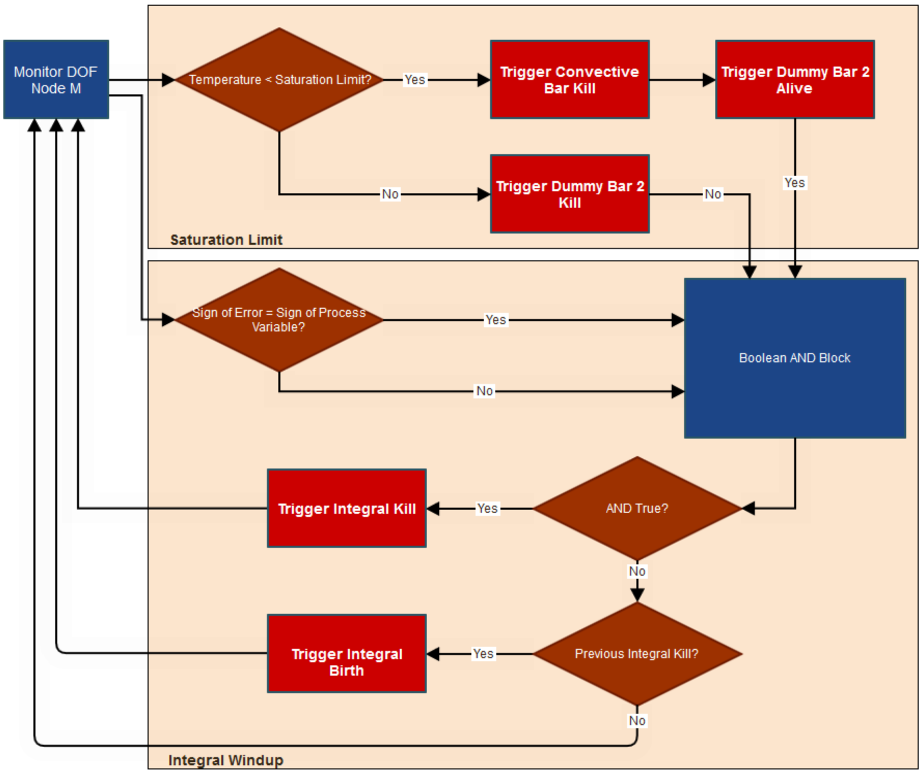

Fig. 4.6 Flowchart of proposed clamping methodology

The procedure makes effective use of dummy convective bars and the element birth and death technique. The approach is divided in two stages: saturation limit and integral windup. A brief description of them is performed below:

- **Saturation limit**

In FEM, the birth and death technique allows elements to be activated or deactivated during the solving process based on degree of freedom (DOF) expressions. In this regard, a vector is defined that correspond to the minimum temperatures that node M can exhibit at the saturation limit of the cooling system. The study is completed by using the same analysis procedure described in the previous section.

- **Integral windup**

An “AND” block is used to check if both saturation limit and equal actuating signal and error signs occurs [K04]. If the condition is true, than the unidirectional element corresponding to the integral controller is killed. Subsequently, a counter is incremented to keep track of this action. The “AND” block is than verified for the next substep. If the condition returns false and the counter indicates that the integral term was previously switched off than the birth function is triggered to turn the unidirectional element back on.

4.7. Ziegler-Nichols Tuning Method

The Ziegler-Nichols method represents a heuristic, iterative and online tuning approach that is intended for design with physical hardware. The methodology comprises 4 stages and proves good results for well-behaved systems:

1) k_i from equation 4.1 is set to an initial small value for the proportional controller (K_p). The integral and derivative terms are switched off;

2) A step load is applied by means of a constant heat flow acting at the base of the fin. The average temperature recorded at the junction between the fin and the heat source is monitored to observe its oscillation;
3) K_p is slowly incremented until neutral stability is achieved ;
4) The value of K_p at neutral stability is considered K_u and the critical period of oscillation is considered T_u (s)

In the next stage, the values of K_p and T_u are used in table 4.1 for identifying K_p and the time constants T_i and T_d [A20].

Table 4.1. Ziegler-Nichols constants

Controller	K_p	T_i	T_d
PID	$0.6K_u$	$T_u/2$	$T_u/8$
PID small overshoot	$K_u/3$	$T_u/2$	$T_u/3$
PID without overshoot	$0.2K_u$	$T_u/2$	$T_u/3$

4.8. LSTM Generalization

In the proposed approach, a LSTM implementation is deployed to generalize the behaviour of the actuating signal (derived during the Equivalent nodal reaction matrix stage) based on the temperatures and heat flow reactions calculated by the FEM solver for 70% of the input data. In this way, the neural model can identify the relationship between the variations of the heat transfer parameters and predict the output of the controller for the remaining 30% of the instruction cycle. In this way, the computational demands of the thermal analysis are lowered.

A dataset is developed comprising a multidimensional array of these features [A12]. The label (or the predicted value) is resembled by the actuating signal. The number of lines and columns corresponding to the 2D shape of the dataset while the 3rd dimension is defined based on a training constant that describes the size of each sequence that is passed to the model (Fig.4.7).

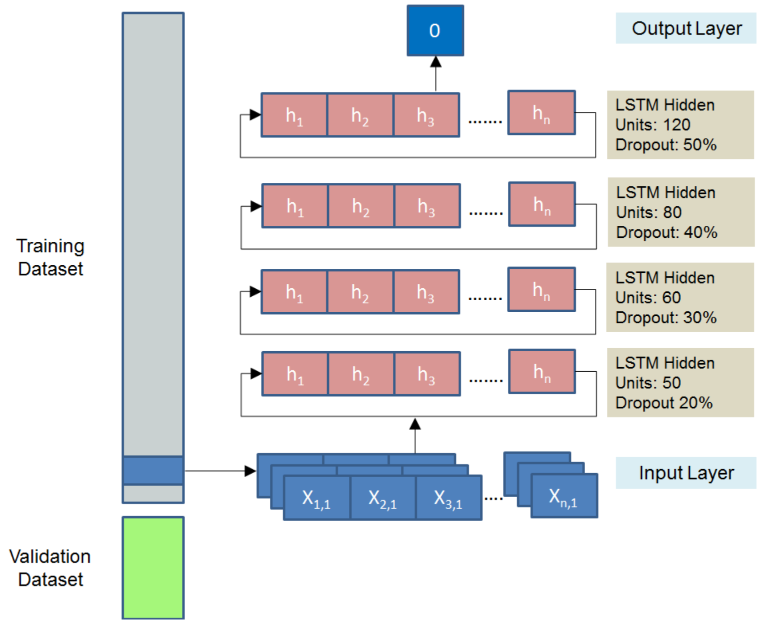

Fig.4.7 Graphical representation of the LSTM architecture

In the proposed model, the input layer consists of a multidimensional array comprising the normalized solver output data. A stack of four LSTM layers is added to capture the abstract concepts in the sequences. The ReLu activation function is used between their outputs. Each hidden layer comprises hidden cells that are characterized by multiple hidden units. On the other hand, each hidden unit addresses the problem of long-term dependencies by adjusting the flow of information with the support of input, output and forget gates.

To improve the generalization ability of the model, the dropout regularization method is deployed to randomly exclude LSTM units during each training step.

Section 3. Case study

A laboratory scale test platform was developed to prove the given concepts. The system in discussion consists of a desktop PC motherboard that is equipped with a single core CPU as the main heat source. Cooling is ensured by means of a vertical plate aluminum alloy heat sink having two axial fans attached. The thermal design solution is subjected to tight space constraints to replicate the conditions occurring in Smart Retrofitting environments. The aim of this setup is to validate the FEM PID Controller by scheduling the actuating signals of the cooling fans. Power and noise efficiency benchmarks are also conducted to evaluate the performance of the proposed solution against a general purpose temperature controller that is integrated in the motherboard. A schematic representation of the hardware deployed is illustrated in Fig. 4.8.

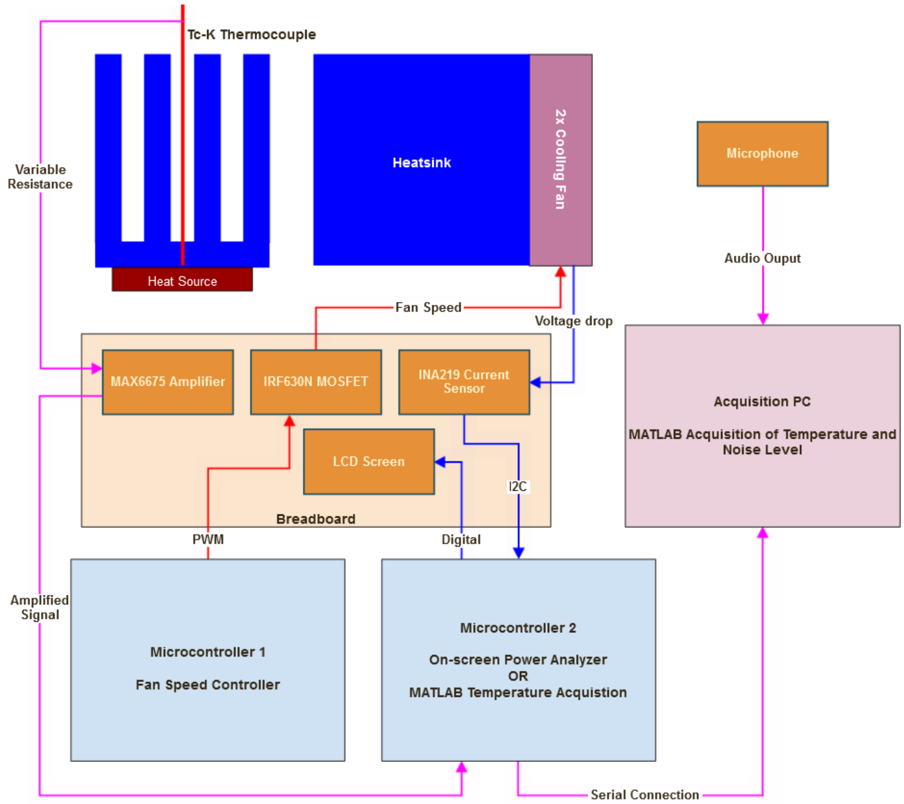

Fig.4.8 Schematic representation of the acquisition system hardware

A description of each constitutive block is detailed below:

- **The heat source:** represents an Intel Pentium 4 Single Core CPU, operating at a frequency of 2800 MHz. At 100% resource usage, the processor has a Thermal Design Power of 50 W.
- **Microcontroller 1**: represents a Mega2560 Arduino Compatible development board. It is used as a Fan speed controller in conjunction with an IRF630N MOSFET. In this regard, one of the digital pins of the microcontroller generates a PWM wave that replicates voltages between 0 and 5V. The on/off pattern of this signal is used to adjust the variable resistance of the MOSFET. Thus, the rotational velocity of both fans is scheduled based on the results derived from the FEM PID controller.

- **Microcontroller 2:** consists of an Arduino Uno development board that has two operational modes: on screen power analyzer (employing an INA219 bidirectional current sensor) and temperature acquisition mode (by means of a TENMA thermocouple operating alongside a Max6675 8-pin SO package).
- **Acquisition PC:** provides the necessary means for programming the microcontrollers as well as performing data acquisition by using MATLAB software. During the experimental procedure, two real-time plots are presented on-screen: the temperature profile of the CPU (by acquiring data from the Max6675 amplifier) and the sound levels of the fans (with the support of an external microphone and the splMeter function deployed in MATLAB).

4.9. Test procedure

The Leibniz formula for π benchmark method is deployed to apply a transient instruction cycle on the CPU by calculating the significant digits of π [B02].

$$\frac{\pi}{4} = \sum_{k=0}^{\infty} \frac{(-1)^k}{2k+1} \tag{4.5}$$

A script was developed to randomly adjust the precision of π value for a time interval of 500 seconds.

The aim of this test procedure is to verify the behavior of both general purpose controller and the proposed FEM PID controller. The value of the set point temperature is defined close to the stable temperature operation limit of the CPU (70°C maximum, 67°C was decided).

4.10. Model simplification

The temperature controller development process is carried out with the support of MSC Patran Finite Element Modeling Software and the LMS Samtech Mecano Thermal solver. The simulation model comprises planar elements that correspond to the 2D plane stress formulation. Only the cross-section of the heat sink profile is considered, the cold plate length being defined as a constant parameter. Half of the total numbers of fins are studied given the symmetry of the geometry. A total of 2856 quadrangular elements are deployed to materialize the profile of the heat sink.

4.11. Definition of unidirectional elements

Three unidirectional elements are deployed with the support of the SAMCEF .MCE DIGI controller. 1D convective bars are employed to link the J node with M [***03]. The area of these elements is equal to 85 mm^2, the value of the film coefficient h_f being considered 600 W/m^2°C. The K nodes are coincident, having applied a temperature BC that corresponds with the set point value of 67°C. The L monitor nodes are also coincident, being attached to the heat flow application area. To recreate the heat removal process that is caused by the air flow, a group of convective bars are deployed adjacent to the unidirectional elements, having defined a section area of 1 mm^2.

4.12. Equivalent nodal reaction matrix

A range of convection film coefficient values are decided by taking into account the minimum and maximum rotational velocity of the cooling fans. For the given test platform, ω_{min} = 2400 RPM and ω_{max} = 9000 RPM. Even so, the experimental setup in discussion can execute low power instruction cycles that demand either fan speeds under the minimum controllable value or the fans to be switched off for the system to reach its set point value. In both scenarios, the forced convection will be replaced by natural convection cooling.

4.13. Element Birth and Death Integral Anti-windup method

The implementation of the Element Birth and Death and Integral Anti-windup method is completed with the support of the Fortran 77 programming language that is embedded in the Samcef solver. Thus, users can develop programs that can run alongside the simulation for applying additional constraints to the model. For this purpose, an external compiler is used to test the code with sample values. In the next stage, the input and output lines are replaced with Samcef commands.

4.14. Ziegler-Nichols Tuning Method

The proportional gain was negatively increased (given the fact that the aim of the controller is the removal of heat from the plant). Figure 4.9 – a depicts the Ku value of -0.35 that is closest to neutral stability. After performing fine adjustments, the full neutral stability of the model is achieved for Ku = -0.3596, the time constant value Tu being estimated at 50 seconds (Fig. 4.9 - b).

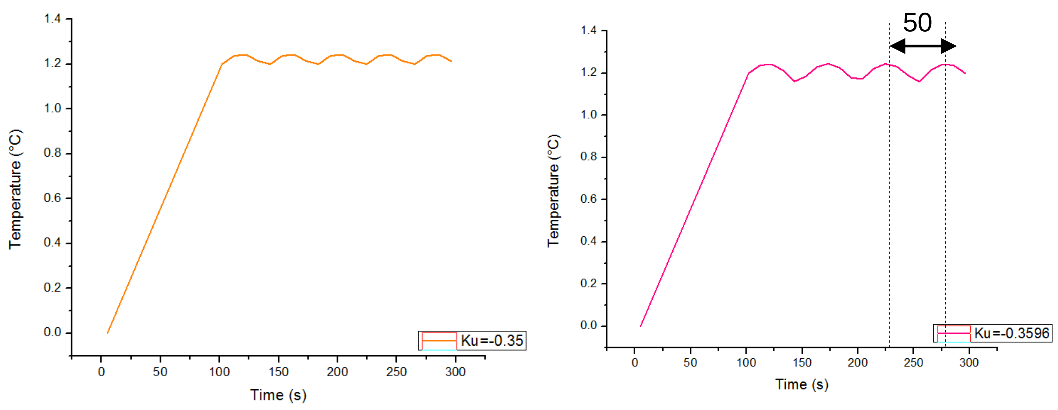

(a) (b)

Fig.4.9 Kp tuning for neutral stability

The resulting values for the controller gains are calculated based on the standard PID constants depicted in: Kp = -0.21576; Ki = -0.0086304 and Kd = -0.0690432

4.15. LSTM Generalization

The LSTM Recurrent neural network is employed to generalize the behavior of the actuating signal calculated at the output of the FEM PID controller. For this purpose, a dataset is developed comprising a wide range of operational scenarios.

The dataset comprises one feature: the heat flow at the base of heat sink (W). The label of the regression process is the actuating signal (as % of the Fan usage). The values are provided as time-series, the step size being 0.01 seconds. Note that values that exceed the power dissipation of the actual CPU were included to enhance the generalization abilities of the model. In total, 90000 rows are provided for training and test purposes (Fig. 4.30).

TensorFlow 2.0 with Keras Machine Learning library is used for defining the LSTM architecture A total number of 5 epochs is chosen as training parameter, meaning that the dataset is backward and forward passed for 5 times. During each epoch, the mean square error loss function is monitored to evaluate the prediction accuracy of the model. At epoch 1, the loss function has a value of 0.0395 while at epoch 5 the value is minimized to 0.0060.

The accuracy of the model is tested by considering a 500 seconds random low power instruction cycle that was not included in the original dataset. This approach was chosen given the fact that it causes sudden spikes of low amplitude in the actuating signal. Figure 4.10 compares the shape of the real and predicted fan speeds for the given inputs.

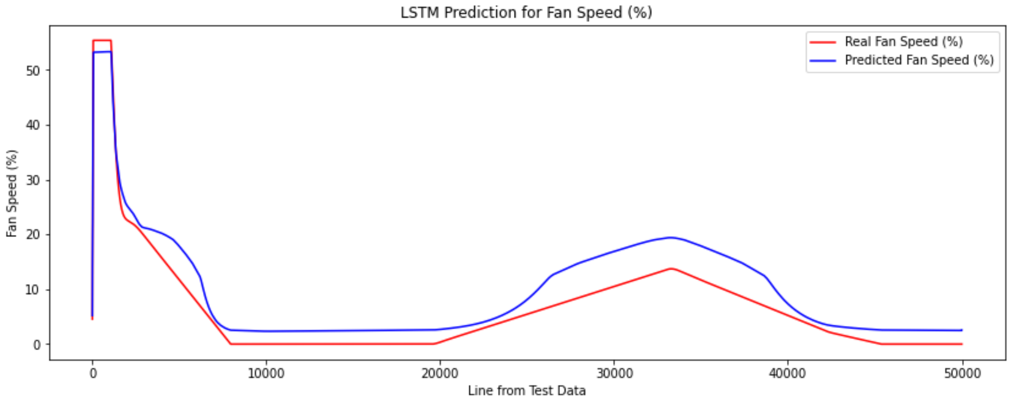

Fig.4.10 The ability of the LSTM neural network to generalize the behavior of the FEM PID controller

4.16. Controller Benchmark

The first stage of the controller benchmark consists of deriving the actuating signal of the cooling fans based on the instruction cycle depicted in section 4.9. The set point temperature is 67°C. In the next stage, the first microcontroller schedules the cooling fans based on the actuating signal while the second microcontroller carries out the data acquisition process.

Power and noise efficiency benchmarks are conducted to evaluate the performances of the controller. For this purpose, the operation mode of the second microcontroller is changed to power measurement. The same procedure is considered for evaluating the performance characteristics of the Smart fan controller that is integrated into the motherboard. In this case, the actuating signal is generated directly at the level of the PWM pins. The set point temperature was increased to 69.2°C to take into account the effect of thermal resistance (given the fact that the smart fan controller operates by acquiring temperature from the internal sensor that is embedded in the CPU die). Figure 4.11 – a and b illustrates the total power draw at 500 seconds for the two control methodologies.

(a)

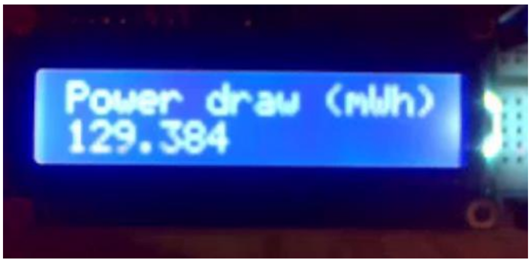

(b)

Fig.4.11. On-screen power draw reading at Δt = 500 seconds

Table 4.2 depicts the noise levels measured by the external microphone for both test scenarios:

Table 4.2 Noise levels for the FEM PID controller

Control methodology	Maximum Noise Levels (dB)	Minimum Noise Levels (dB)	Average Noise level (dB)
FEM PID Controller	26.67	12.23	23.66
Smart Fan Controller	27	13.51	25.88

Figure 4.12 compares the FEM PID and the Smart fan controller temperature curves.

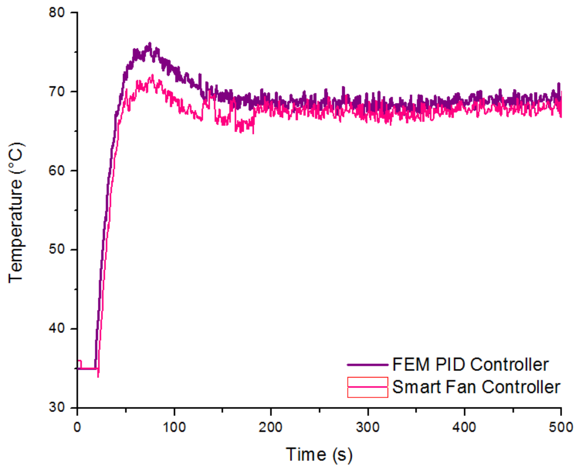

Fig. 4.12. FEM PID and Smart Fan controller experimental temperatures

The comparison of the performance characteristics of the two controllers is carried out in table 4.3. The highlighted values are better ones.

Table 4.3 Comparison of controller performances

Characteristics	FEM PID Controller	Smart Fan Controller
Rising time (s)	50	**30**
Settling time (s)	150	**100**
Overshoot (%)	12	**5**
Power Draw (mWh)	**107.676**	129.384
Avg. Noise level (dB)	**23.66**	25.88

A cross validation is completed between the simulated and predicted FEM PID controller. For this purpose, the previously considered instruction cycle is used as input heat flow in the thermal analysis. The actuating signal derived by the simulation is employed to schedule the cooling fans in the real-world system. Figure 4.13 depicts the two temperature curves.

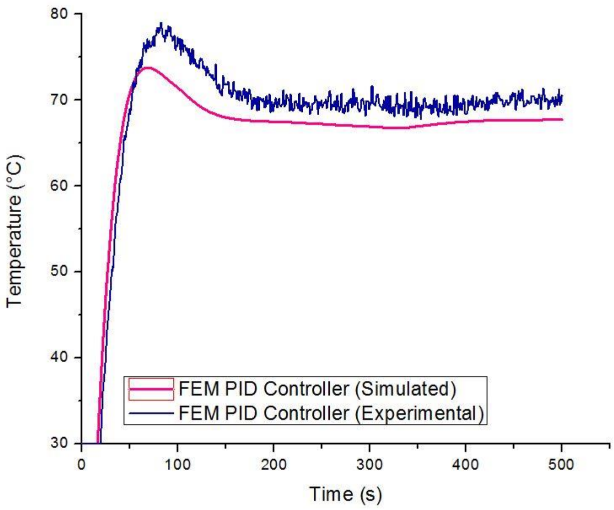

Fig. 4.13 Cross-validation experimental vs. simulation temperature curves

The results achieved indicate divergences of +6.11% in case of the power draw and -7.21% in case of the average noise levels.

Section 4. Conclusions

The present chapter addresses the limiting aspects of the embedded systems cooling workflows with emphasize on the temperature controller development process. Formalization of this methodology is achieved by re-using the simulation models that were previously completed in the thermal design stage. The issues related to the computational demands of FEM PID controllers are tackled by reducing the dimensionality of the heat transfer problem. A simulation approach that is based on lumped parameter heat transfer modeling and user-defined subroutines is proposed to facilitate the real-world implementation of the control methodology. The generalization of the approach is achieved by means of LSTM RNNs.

The original contributions of the work can be grouped in the following categories:

1. **Theoretical contributions**: the development of a PID temperature controller with saturation limit and integral windup method and its implementation in a FEM simulation environment.
2. **Methodological contributions**: the conversion of the lumped process variable at the output of the controller in a meaningful signal by means of an equivalent convection matrix approach; the tuning of the controller gains by employing the Ziegler-Nichols heuristic method and the generalization of the actuating signal based on a single input, single output LSTM model.
3. **FEM Modelling original contributions**: the model simplification approach based on dimensionality reduction and definition of symmetry BCs.
4. **CAE implementation:** An original SAMCEF-Patran original implementation was completed.
5. **Experimental procedure:** the development of the experimental test platform and post-process of the results.

The findings of the research were published in:

- **Alexandru, T. G.,** & Pupaza, C. (2021). The development of PID temperature controllers based on FEM thermal analysis. In MATEC Web of Conferences (Vol. 342). EDP Sciences, Indexing in progress.

By tackling both thermal design and control engineering issues of smart retrofitting projects, the proposed approach can facilitate the development of cooling solutions for smart retrofitting projects with minimized knowledge and resource usage. Even so, the materials required for developing heat sinks as well as the unpredictable obsolescence of embedded systems in the context of Industry 4.0 brings into discussion arising environmental concerns. Such issues are addressed in Chapter 5 of the work.

Section 1. Sustainability in thermal design processes

5.1. General aspects

Thermal design represents a vital subsystem of newly developed or retrofitted computer control units. The resulting assembly of cooling components has the aim of removing the power dissipated by the active heat sources. In this way, the safe and reliable operation of shop floor devices is ensured throughout their entire life cycle. The wide range of materials employed in thermal design, the complexity of the manufacturing technologies required to develop heat sinks and the pumping power resulting from the operation of forced convection cooling solutions bring into discussion arising environmental issues (Fig. 5.1).

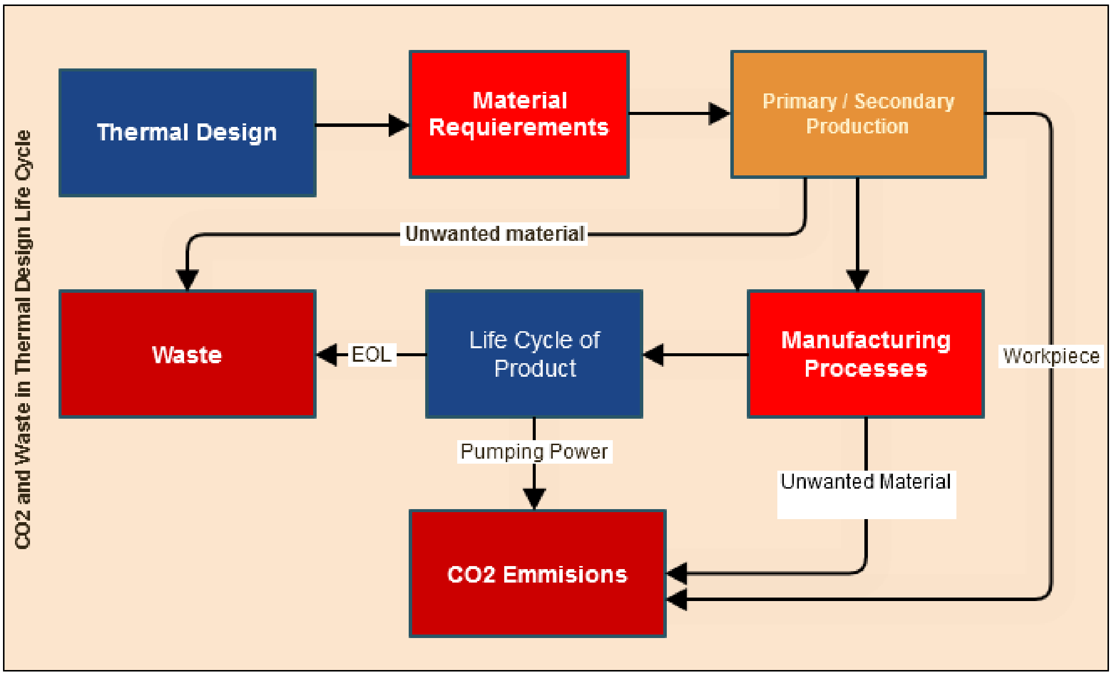

Fig. 5.1 CO_2 emissions and waste resulting from the life cycle of thermal design solutions

In the design stage, engineers decide the optimal geometric specifications of the cooling components and the range of fans or blowers that are required to enhance power removal [L09]. The manufacturing of heat sinks demands the extensive use of non-ferrous materials billets. Most of the times, extrusion, high pressure casting or milling technologies are employed to transform the raw material into various shapes of cooling fins [E02]. The energy and tools required to complete this process represents a source of CO_2 emissions and waste [A07]. Furthermore, carbon footprints also occur due to the primary and secondary production of the workpieces as well as the operation of the cooling fans.

Another environmental issue of thermal design is emphasized in the present industrial context by the unpredictable obsolescence of the embedded systems that are deployed in the computer control units of smart devices [M05]. In this regard, new hardware solutions emerge to the market every year to support the increasing computational demands of the Industry 4.0 transformative technologies. From this point of view, devices that are considered in the growth life cycle stage are phased out. To be competitive, companies continuously improve the resources of shop floor devices. As a consequence, electronic waste and CO_2 emissions emerge, demanding appropriate End-of-Life (EOL) strategies.

5.2. Theoretical considerations

An example of waste and carbon footprint calculation is provided below by considering a heat sink comprising non-equal height fins that is manufactured by milling a 70x100x100 mm aluminum sheet. The geometric specifications of the solution are depicted in figure 5.2.

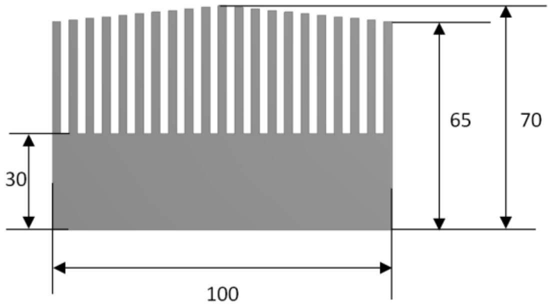

Fig.5.2 The geometric specifications of the heat sink

The benchmark procedure is carried out by evaluating in the first stage the CO_2 emissions resulting from the workpiece manufacturing process. All information is extracted from [G05] by considering the Bayern-Hall Héroult Route process for the primary production of aluminum as well as the secondary production of aluminum by means of remelting and casting scrap material.

In average, 26.38 $KgCO_2$ are released into the atmosphere for manufacturing the aluminum sheet workpiece by primary production or 1.19 $KgCO_2$ by secondary production means.

The milling process carbon footprint is evaluated in the next stage. For this purpose, the net power (P_C) and machining time (T_c) requirements are derived from the cutting parameters [I04]:

$$P_C = \frac{a_e \cdot AP \cdot V_f \cdot k_c}{60 \cdot 10^6} \tag{5.1}$$

Where a_e represents the radial depth of cut (mm), AP the axial depth of cut (mm), V_f represents the table feed (mm/min) and k_c represents the specific cutting pressure (N/mm^2)

$$T_C = \frac{l_m}{V_f} \tag{5.2}$$

Where l_m represents the machining length (mm).

The total energy requirements (KWh) are calculated by multiplying the net power (KW) by the machining time (h) for each milling feature (i):

$$P_{total} = \sum P_{c_i} \cdot T_{C_i} \tag{5.3}$$

In most of the cases, milling machines convert electrical into mechanical energy. Therefore, the carbon footprint of the process can be estimated from P_{total} by considering the average 0.56 KgCO2/KWh emission factor derived from [***01].

Sandvik CoroPlus tool guide is used to calculate the cutting parameters. A 28 KW machining center is considered comprising an 18000 RPM spindle. The workpiece used is a 90 HB hardness general purpose aluminum alloy. In total, 0.0250 $KgCO_2$ are released into the atmosphere for milling the fins and finishing the base of the heat sink.

In the next stage, the carbon footprint resulting from the operation of the cooling fan is estimated for a 10000 hours life cycle. For this purpose, an 80 mm fan running at an average speed of 2000 RPM with a 24 CFM air flow is considered. Based on the datasheet of the product, the instantaneous power consumption of the fan is 0.069W (derived from V_{ce} and I_c). Thus, the carbon footprint for 10000 hours can be estimated as 0.22 KgCO2.

The results of the benchmark process indicate that over 99% of the carbon footprint occurs due to the primary production of the workpiece. In this regard, a sustainable product development approach for thermal design should focus on limiting the amount of materials deployed. Even so, a more effective workaround consists of the partial or complete replacement of aluminum or copper alloys with alternative or greener materials. The limiting aspect of this perspective is the fact that not all existing alternatives facilitate the manufacturing of heat sinks as one single component. Furthermore, the long term exposure to cooling fluids and the increase and decrease of the heat source temperature limits the range of available solutions.

Section 2. The proposed approach

The objective of the present chapter is to study the perspective of integrating alabandite, a manganese sulfide that is widespread throughout the tailings of Au-Ag-Te mining facilities in the design of forced convection heat sinks.

5.3. Mineralogical and geological aspects

In Romania, significant concentrations of alabandite can be found in the tailings surrounding the Săcărâmb Au-Ag-Te (type locality) and in Baia de Arieș polymetallic ore deposits [D07]

Sulfosalt tailings represent a worldwide environmental concern due to the oxidability and solubility of such minerals [D03, P07]. From this point of view, the long term exposure of alabandite to air or water dissociates manganese and sulfur causing groundwater pollution. In this regard, finding an economic viability for this material can tackle multiple issues.

5.4. Schematic representation of the methodology

The proposed approach for integrating alabandite in the thermal design processes comprises 4 layers of abstraction:

1) **Evaluation of toxicity hazard:** alabandite brings into discussion toxicity hazards to the dissociation of manganese and sulfur in long term exposure to air or water. From this perspective, this raw material cannot be deployed in thermal design processes, in particular in forced convection cooling systems. Even so, one workaround for limiting the solubility and oxidability of sulfosalts consists of coating their exterior surfaces with a protective primer.
2) **Thermal characteristics:** the study carried out in the previous sections proves that the thermal conductivity of the materials employed in the thermal design process have a great influence on the overall fin cooling efficiency. In this regard, the thermal characteristics of alabandite are analyzed by experimental means to identify if the sample is a semiconductor, conductor or insulator. It is also important to study the influence of the protective coating on the thermal characteristics of the material.
3) **Cooling system development process:** due to its isometric crystal system, alabandite can only be processed by means of cold saw cutting technology in rectangular shape bodies. Depending on the desirable thermal resistance, a standalone alabandite rectangular heat sink can be developed. When a more significant amount of power is dissipated by the heat source a hybrid material bonded heat sink can be deployed by combining alabandite with a thin sheet metal body. This scenario is only applicable to forced convection cooling systems.

4) **Optimization:** the objective of the proposed sustainable product development approach is to maximize the integration of alternative materials in the thermal design process. For this purpose, the heat sink design derived in the previous layer is subjected to computational fluid dynamics studies to identify the optimal pattern sequence of the alabandite bodies. The results achieved are used for implementing the final design.

A schematic representation of the approach is depicted in figure.5.3

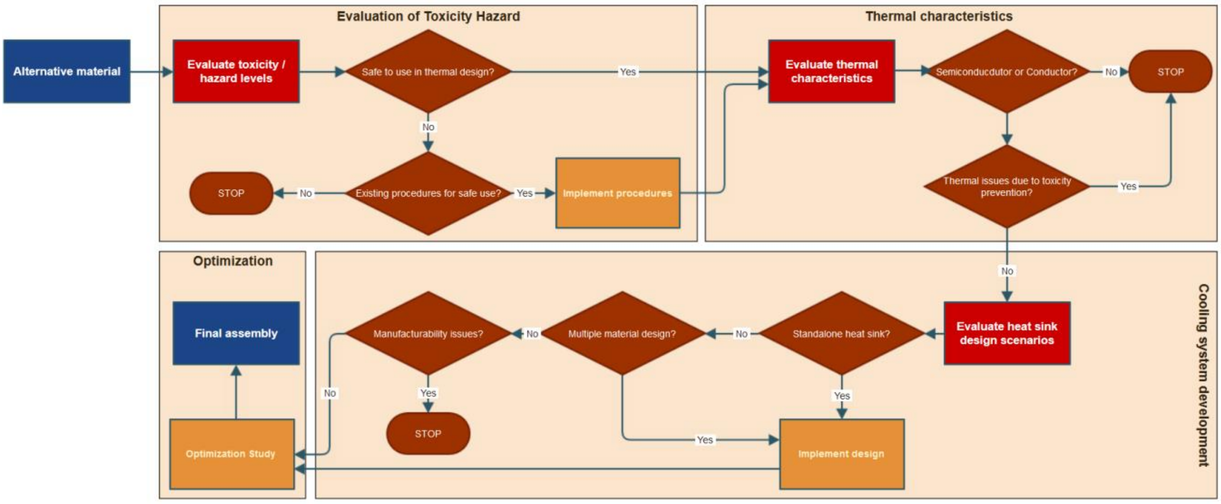

Fig. 5.3 Schematic representation of the proposed approach

Section 3. Case study

The given concepts are proved by means of an experimental setup that comprises a constant power heat source and a forced convection cooling system (Fig. 5.4).

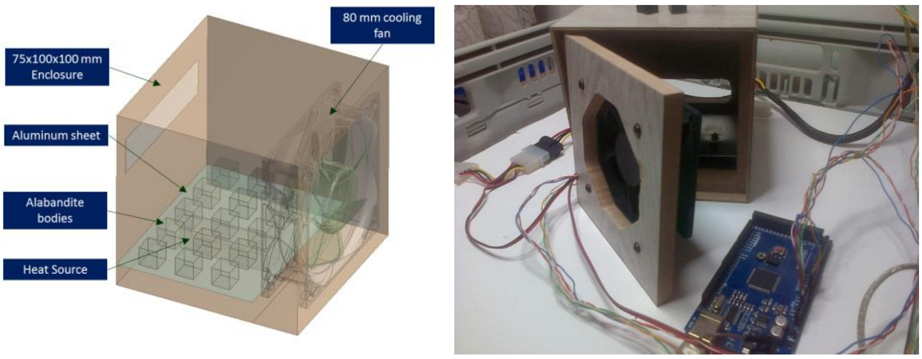

Fig.5.4 Forced convection cooling system

A bonded heat sink design is deployed to maintain the temperature of the active component below its operational limits. The fins of the design solution are materialized by rectangular alabandite bodies. The flow of air is ensured by an intake fan mounted on the front side of the enclosure.

5.5. Evaluation of toxicity hazard

To limit the side effects of alabandite oxidability and solubility, an acrylic primer is applied by means of a pneumatic paint gun to coat the exterior surfaces of the material. One known issue of acrylic paints is their low thermal conductivity given the fact that the base component of such products is an insulator thermoplastic [C04]. From this point of view, a substantial decrease of the alabandite thermal resistance is expected. To overcome such issues, the baseline primer is mixed with graphite powder. The ratio is decided as 1/4 with 10% viscosity thinner for ensuring the flow of the resulting mixture through the nozzle of the pneumatic gun. In this way, the graphite powder sticks to the surfaces of the alabandite body enhancing its thermal contact conductance while the layer of primer ensures optimal protection from oxidability and solubility (Fig. 5.5).

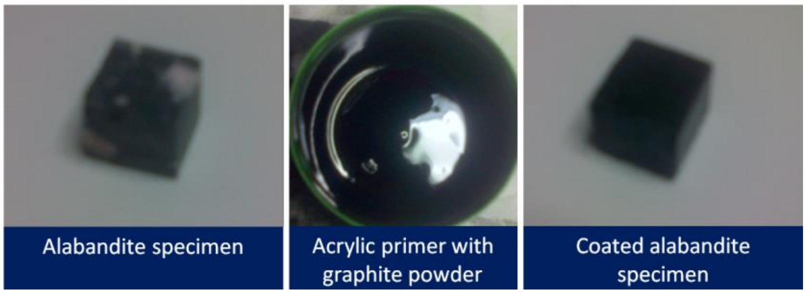

Fig. 5.5. Baseline and coated alabandite sample

5.6. Thermal characteristics

The density of the alabandite sample is derived from the mass of the sample: $9.5 \cdot 10^{-4}$ Kg for a volume of 250 mm^3, resulting a density of $3.8 \cdot 10^{-9}$ t/mm^3.

An experimental setup is developed to evaluate the thermal characteristics of the baseline and coated alabandite specimens (Fig. 5.6).

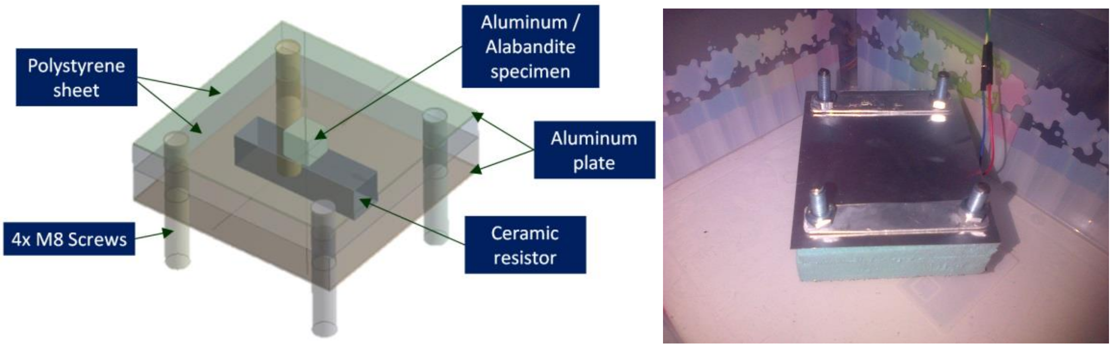

Fig. 5.6. The experimental setup for evaluating the thermal characteristics

The test platform comprises two polystyrene sheets that embed a constant power dissipation ceramic resistor and a square sample of the analyzed material. The two bodies are in contact one to another, a thermal gradient occurring at their junction surfaces. The assembly is held together by two aluminum plates to ensure the optimal conductance. Four M8 screws are deployed to secure the assembly in place. A temperature gradient occurs between the upper surface of the resistor and the top aluminum plate. The thermal conductivity of any specimen can be evaluated based on Fourier's law of conduction by measuring the cold plate temperature. On the other hand, a transient thermal analysis can be carried out to approximate the specific heat of the studied material based on the Direct Optimization procedure implemented in the Workbench interface [***02].

A summary of the thermal characteristics derived for a pure alabandite sample is emphasized below:

- Density: $3.8 \cdot 10^{-9}$ t/mm3
- Thermal conductivity: 0.718 W/m°C
- Specific heat: 251.92 J/Kg°C

In the next stage, the thermal characteristics are evaluated for the coated alabandite sample. Only a minor change of the initial values occurs:

- Density: $3.8 \cdot 10^{-9}$ t/mm3
- Thermal conductivity: 0.803 W/m°C
- Specific heat: 303 J/Kg°C

5.7. Cooling system development

Coated alabandite bodies can be deployed as standalone coolers in low power applications that demand high thermal resistance values. Even so, a more effective use of this material can be achieved by developing bonded heat sinks. In this regard, a thin aluminum sheet can be used as a cold plate for gluing alabandite cubes to act as fins (Fig. 5.7).

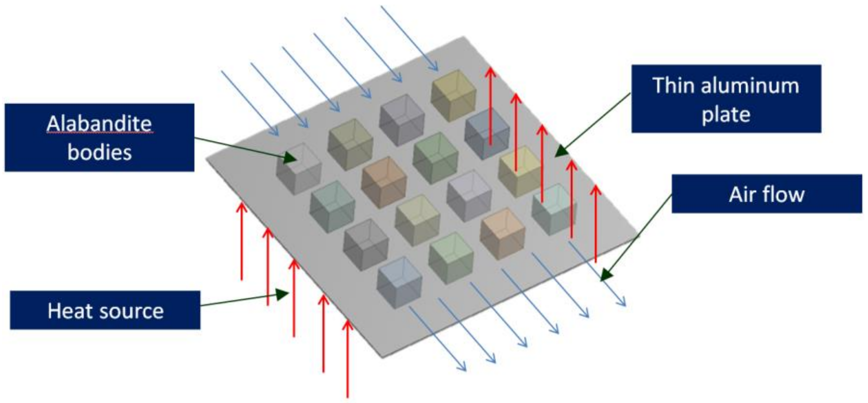

Fig. 5.7. Virtual prototype of the bonded heat sink design

In this way, the path of the air flow is constrained by the existence of additional walls in the enclosure domain. As a consequence, a local increase of the cooling fluid velocity occurs in the proximity of the alabandite bodies, resulting enhanced convective heat transfer. This behavior can be emphasized by means of a computational fluid dynamics study carried out by using ANSYS Fluent. For this purpose, a 100x100 square aluminum plate is subjected to a 0.5m/s air flow, with the Reynolds number in the laminar domain. In the same problem, a 10x10 mm alabandite body is added in the centroid of the plate. In this case the fluid flow is characterized by a turbulent behavior, the solving process being carried out by using the k-ε model. A clear change can be noticed in the streamline between the initial and updated configurations (Fig. 5.8 – a and b).

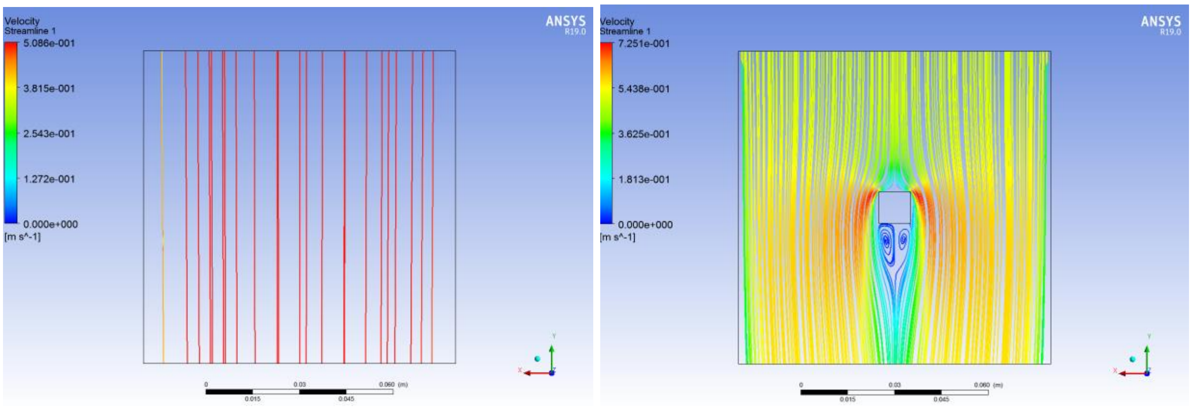

(a) (b)

Fig. 5.8 The change of the velocity streamline considering the laminar flow regime

In the laminar case, the velocity of the cooling fluid is equal between the inlet and outlet. On the other hand, a substantial increase of 50% in the air velocity can be noticed in the turbulent regime case due to the presence of the vertical walls in the centroid of the plate.

In this regard, the rectangular alabandite bodies can be deployed to constrain the air flow. Furthermore, their semi conductive capabilities will also contribute to the dissipation of heat from the cold surface.

5.8. Optimization study

One objective in the development of this alternative heat sink design consists of identifying the optimal pattern sequence of the fins to ensure optimal cooling. A response surface study is conducted for the problem described earlier to identify the appropriate design scenario. For this purpose, the horizontal and vertical geometry constraints of the body are parameterized. The output variable represents the maximum temperature that occurs on the cold plate under a constant power dissipation of 0.5W. Figure 5.9 depicts the resulting response surface.

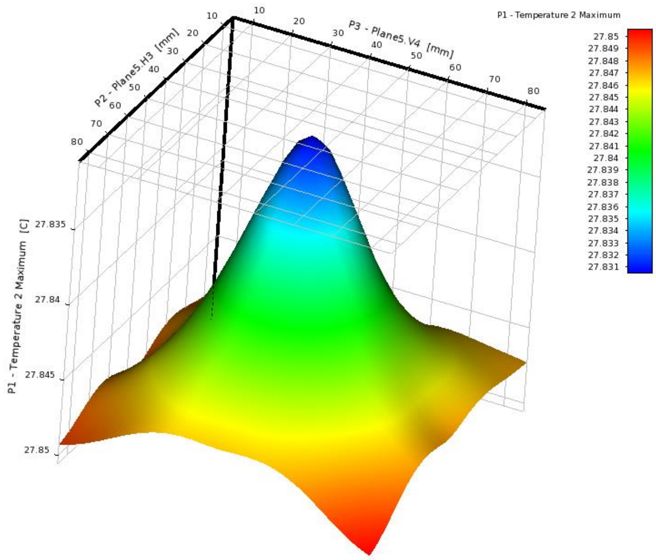

Fig. 5.9 XY Location of the alabandite sample vs. the cold plate temperature increase

The results highlight the fact that the optimal cooling capabilities are achieved when the alabandite bodies are deployed in the centroid of the cold plate, the temperatures being 0.07% lower than compared to any other scenarios. This can be explained by the velocity gradient from figure 5.8 which emphasize a wide area of maximum values that are equally distributed in the left and right corners of the rectangular alabandite body.

5.9. Implementation of the given concepts

The results and conclusions derived in the previous sub-sections are used for implementing the given concepts in the forced convection cooling system depicted at the beginning of this section. In this regard, a simulation study is carried out to replicate the behavior of the test platform. ANSYS Icepak is used for this purpose. The simulation model includes 9 alabandite bodies that are positioned in the centroid of the cold plate. The size of the samples used is 10x10x10 mm. the existence of the alabandite bodies constrains the air flow, enforcing its velocity to increase in the proximity of opposite vertical planes (≥1.59 m/s). As a consequence, the forced convection cooling capabilities are enhanced. The velocity vectors and the temperature profile fringes are depicted in figure 5.10.

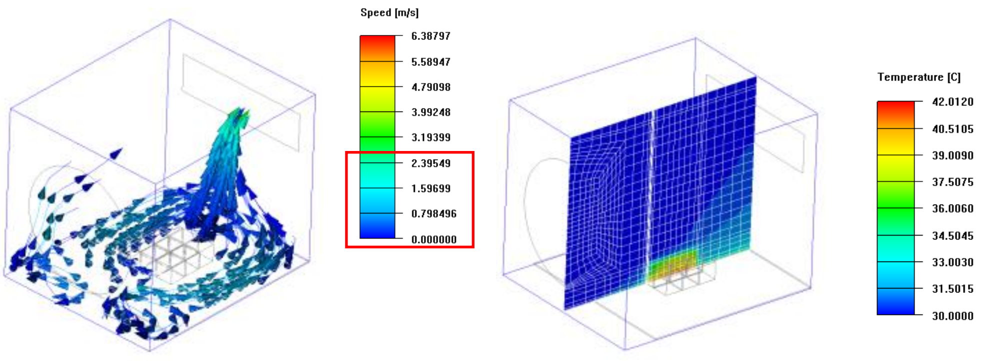

Air Speed – 6.38 m/s *Temperature – 42.5°C*

Fig. 5.10 Air speed and temperature profile for the bonded heat sink scenario

The results of the simulation are verified by means of the real-world experimental setup (Fig. 5.11).

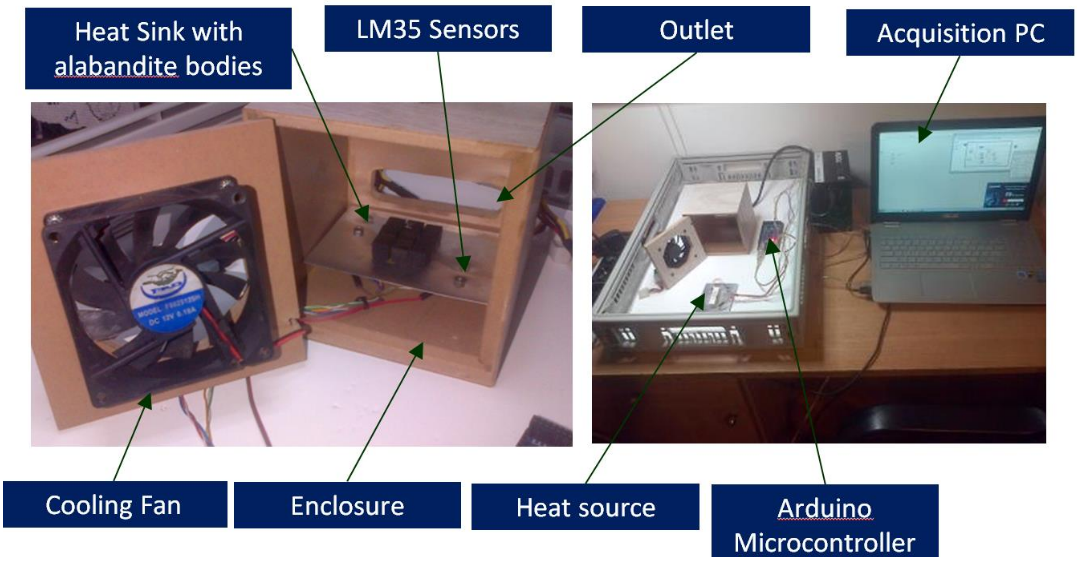

Fig. 5.11 The experimental setup used to verify the simulation results

For this purpose, two LM35 sensors are deployed in two opposite corners of the cold plate. An Arduino Mega 2560 compatible microcontroller is used for temperature acquisition. Figure 5.12 depicts the two analyzed cooling solutions with emphasize on the location of the heat source and measurement system.

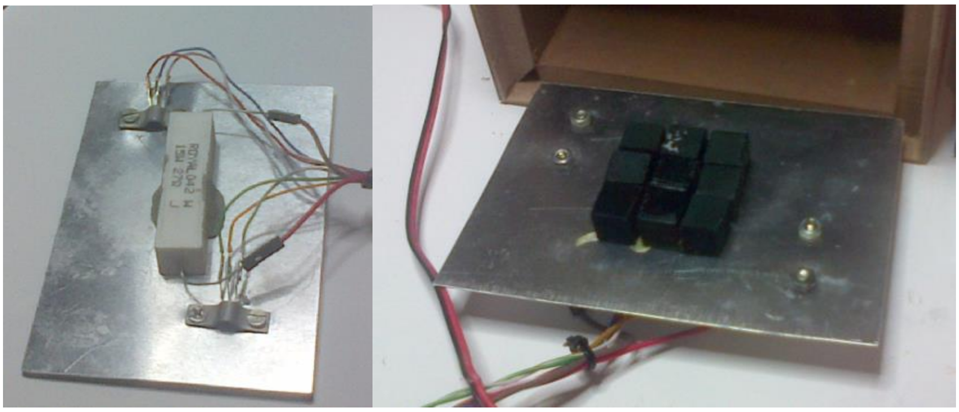

Fig. 5.12 Bonded heat sink comprising a thin aluminum plate and 9 alabandite bodies

The test cycle is decided at 1000 seconds for the system to achieve steady-state. The average value of the signals derived from the two sensors is considered. Figure 5.13 illustrates the time vs. temperature plot for the cold plate cooling scenarios.

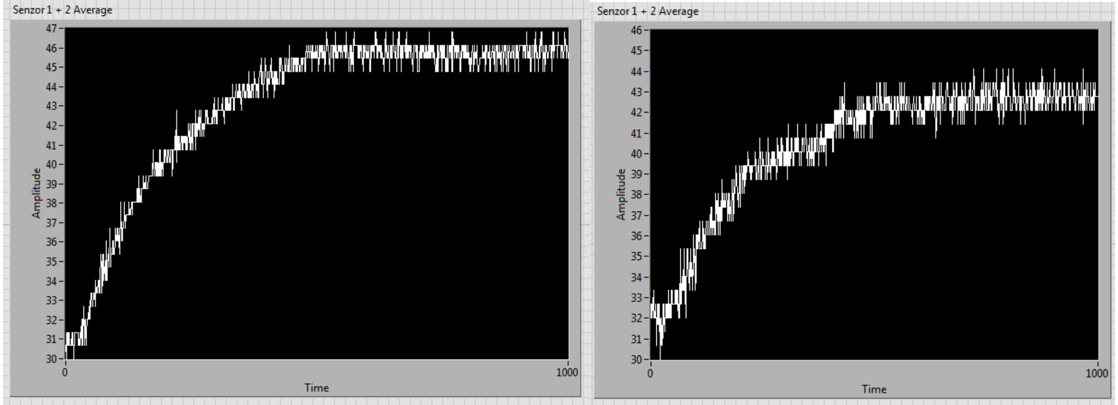

Fig. 5.13 Time vs. temperature graph for the cold plate cooling scenario

The equilibrium temperature is estimated at 46°C.

In the next step, the behavior of the bonded heat sink design is evaluated by employing the same procedure. The equilibrium temperature is estimated at 43.5°C.

5.10. Carbon footprint savings

In the next stage, the alabandite fines are replaced with vertical aluminum plates. Their geometric specifications are derived with the support of the analytical methodology depicted in [L08]. Information regarding the Reynolds number and the heat transfer coefficients occurring due to the turbulent flow regime is extracted from the cold plate simulation.

The same carbon footprint benchmark procedure that was previously completed in section 2 is employed to identify the CO_2 emissions resulting from the workpiece production, fins manufacturing and pumping power of the vertical plate heat sink. In total, 2.38 $KgCO_2$ are dissipated in case of primary production and 0.30 $KgCO_2$ in case of secondary production.

The carbon footprint of the cold saw cutting technology employed for manufacturing the alabandite fins is estimated by experimentally measuring the power requirements of the process. In this regard, a 35x15x1 mm alabandite body is processed on a Struers Accutom-5 precision machine (Fig. 5.14 – a and b).

(a) (b)

Fig. 5.14 (a) Steuers Acutom 5 precision cutting and grinding machine; (b) the alabandite specimen

The measurements were completed at the Geological Institute of Romania. Energy requirements of the cutting process are measured using an Orno OR-WAT-419(GS) outlet socket energy meter (Fig.5.15).

Fig. 5.15 Orno OR-WAT-419(GS) power meter

For the cutting time of 0.05 hours, the maximum instantaneous power consumption is 0.158 KW. Thus, the total power required to process 5250 mm^2 of alabandite is 0.008 KWh or $1.52 \cdot 10^{-6}$ KWh for each mm^2. In case of the bonded heat sink, the 9 alabandite fins have a total volume of 9000 mm^2. In conclusion, the total power required for manufacturing the fins is 0.0137 KWh or 0.00152 KWh for each fin.

Carbon savings of up to 78% can be achieved in case of primary production and 16% in case of secondary production workpiece materials. For information, table 5.1 represents the detailed percentage changes for the manufacturing of the two heat sinks.

Table 5.1. Detailed percentage changes for the two heat sinks

<table>
<tr><th rowspan="2">Workpiece</th><th colspan="2">Carbon footprint ($KgCO_2$)</th><th rowspan="2">Difference (%)</th><th rowspan="2">Fins manufacturing</th><th colspan="2">Carbon footprint ($KgCO_2$)</th><th rowspan="2">Difference (%)</th></tr>
<tr><th>Baseline Heat Sink</th><th>Bonded Heat Sink</th><th>Baseline Heat Sink</th><th>Bonded Heat Sink</th></tr>
<tr><td>Primary Production</td><td>2.13</td><td>0.28</td><td>-87.02</td><td>Primary Production</td><td rowspan="2">0.0277</td><td rowspan="2">0.0243</td><td rowspan="2">-12.28</td></tr>
<tr><td>Secondary Production</td><td>0.05</td><td>0.01</td><td>-87.02</td><td>Secondary Production</td></tr>
</table>

The results achieved prove that significant carbon savings (up to 1.85 Kg CO_2 for the present study) can be achieved by integrating alabandite as an alternative solution for designing cooling fins in forced convection heat sinks. Furthermore, the economic viability of this material can have long term positive effects on the populations that are impacted by manganese pollution.

Section 4. Conclusions

The present chapter addresses the environmental issues of the thermal design process in the present industrial context. Three main sources of CO_2 emissions are emphasized throughout the work: the production of workpieces for heat sinks, the machining of cooling fins and the pumping power of fans or blowers. The objective of a sustainable product development approach that is applicable to thermal design processes is highlighted by the minimization of the material requirements. In this regard, the proposed approach investigates the ability of integrating alabandite in the design of bonded heat sinks for use in forced convection environments. In the first stage, the toxicity issues of the material are addressed by coating its exterior surfaces with an acrylic primer that is mixed with graphite powder. An experimental setup is developed to evaluate the thermal characteristics of the baseline and coated alabandite specimens. The results achieved indicate that alabandite is a semiconductor. Also, the coating applied on the external walls has no significant effect on the thermal characteristics of the material. A hybrid material design is proposed comprising a thin aluminum cold plate with glued alabandite cubes. The optimal pattern sequence of the fins is decided with the support of the response surface methodology. The study highlights the fact that optimal cooling is achieved when the additional bodies are positioned in the proximity of the cold plate centroid. The given concepts are proved by means of a real-world forced convection cooling setup by comparing the performances of the cold plate vs. the bonded heat sink. This is achieved with the support of computational fluid dynamics simulations and experimental procedures. A comparison between the proposed bonded heat sink and a conventional vertical plate design is included for emphasizing the carbon savings of the approach.

The original contributions of the work can be grouped in the following categories:

1. **Theoretical contributions**: the estimation of CO2 emissions resulting from the life cycle of thermal design solutions.
2. **Methodological contributions**: the development of an acrylic coating system for minimizing the toxicity of alabandite ; the design of a bonded heat sink comprising alabandite fins for forced convection cooling
3. **FEM Modelling original contributions**: the evaluation of the thermal characteristics of alabandite based on experimental and simulation procedures
4. **CAE implementation:** An ANSYS Mechanical and Fluent original implementations were completed.
5. **Experimental procedure:** the development of two experimental platform and post-process of the results.

The findings of the research were published in:

- **Alexandru, T.G.** & Pupaza, C. (2017), “Eco-design of heat sinks based on CAD/CAE techniques”, Proceedings in Manufacturing Systems, Vol.12, Iss.1, pp. 9-16, 2017.

Future work will focus on minimizing the specific heat error by improving the experimental procedure. Another future objective of the research consists of evaluating the potential of using nano-powders as an alternative coating technology.

Final conclusions

Smart retrofitting represents an alternative industrial transformation approach that aims upgrading the obsolete computer control units of shop floor devices. In this way, conventional automation can be converted into CPS with the support of additional hardware platforms. This process benefits from a wide variety of computer aided software as well as high level application programming interfaces. Even so, a limited range of workflows bring into discussion custom tailoring issues given the peculiarities of each computer control unit and the surrounding industrial ecosystem. In this regard, the cooling of embedded systems represents a limiting aspect of the smart retrofitting projects. This is due to the emerging space, power and environmental constraints. In this regard, a breakdown of the underlying disciplines of the process is carried out. A practical example is provided from the begining of the work to emphasize the literature gap of embedded systems cooling in the present industrial context.

The total heat transfer rate evaluation process represents an essential stage of any thermal design process. While conservative approaches exist, their use in smart retrofitting is limited given the tight space and power constraints. To overcome such issues, a lumped parameter model is developed based on the theoretical considerations of first order systems. The given concepts are transposed to a FEM simulation environment with the support of variable conductance and capacitance macro elements. The parameterization of the thermal analysis is achieved by means of experimental data. Experiments are also conducted throughout the work to prove the practical use of the approach for evaluating the thermal behavior of standalone heat sources. The methodology can successfully be re-used when the package was previously studied. Alternatively, a coarse description of the total heat transfer rate can be achieved by extrapolating the results for new electronic components.

Describing the total heat transfer rate in multi-chip electronic components represents a challenging perspective due to the complexity of the underlying thermal networks. In this regard, the proposed lumped parameter methodology proves of limited use given the extended number of experimental variables required for parameterizing the model. Furthermore, the initial finite element model is only able to study each heat generating location at a time. To overcome such issues, the practical use of ML is proposed as a tool for predicting the temperature gain and time constants based on the technical and performance specifications of the studied package. Changes are included in the initial simulation model to take into account the additional junctions.

The limiting aspects of the embedded systems cooling workflows are discussed with emphasize on the temperature controller development process. Formalization of this methodology is achieved by re-using the simulation models that were previously completed in the thermal design stage. The issues related to the computational demands of FEM PID controllers are tackled by reducing the dimensionality of the heat transfer problem. A simulation approach that is based on lumped parameter heat transfer modeling and user-defined subroutines is proposed to facilitate the real-world implementation of the control methodology. The generalization of the approach is achieved by means of LSTM RNNs.

The environmental issues of the thermal design process are presented in the actual industrial context. Three main sources of CO_2 emissions are emphasized throughout the work: the production of workpieces for heat sinks, the machining of cooling fins and the pumping power of fans or blowers. The objective of a sustainable product development approach that is applicable to thermal design processes is highlighted by the minimization of the material requirements. In this regard, the proposed approach investigates the ability of integrating alabandite in the design of bonded heat sinks for use in forced convection environments. In the first stage, the toxicity issues of the material are addressed by coating its exterior surfaces with an acrylic primer that is mixed with graphite powder. An experimental setup is developed to evaluate the thermal characteristics of the baseline and coated alabandite specimens. The results achieved indicate that alabandite is a semiconductor. Also, the coating applied on the external walls has no significant effect on the thermal characteristics of the material. A hybrid material design is proposed comprising a thin aluminum cold plate with glued alabandite cubes. The optimal pattern sequence of the fins is decided with the support of the response surface methodology. The study highlights the fact that optimal cooling is achieved when the additional bodies are positioned in the proximity of the cold plate centroid. The given concepts are proved by means of a real-world forced convection cooling setup by comparing the performances of the cold plate vs. the bonded heat sink. This is achieved with the support of computational fluid dynamics simulations and experimental procedures. A comparison between the purposed bonded heat sink and a conventional vertical plate design is included for emphasizing the carbon savings of the approach.

The original contributions of the Doctoral Thesis can be summarized as

1. **Theoretical contributions**:
    - The use of first order systems with adjustable temperature gain and time constants for developing a lumped parameter input-output model.
    - The development of a Visual Basic application tool for the automated parameterizing of lumped parameter models based on experimental data.
    - The development of a PID temperature controller with saturation limit and integral windup method and its implementation in a FEM simulation environment
    - The estimation of CO2 emissions resulting from the life cycle of thermal design solutions.
2. **Methodological contributions**:
    - The development of experimental procedures for system identification purposes and the further use of the results for parameterizing transient thermal analysis.
    - The extension of the original lumped parameter simulation model to include multiple thermal junctions.
    - The conversion of the lumped process variable at the output of the controller in a meaningful signal by means of an equivalent convection matrix approach.
    - The tuning of the controller gains by employing the Ziegler-Nichols heuristic method.
    - The generalization of the actuating signal based on a single input, single output LSTM model.
    - The development of an acrylic coating system for minimizing the toxicity of alabandite.
    - The design of a bonded heat sink comprising alabandite fins for forced convection cooling.
3. **FEM Modeling original contributions**:
    - The practical use of a macro element for lumped parameter modeling based on temperature dependent conductance and capacitance.
    - The extension of the original lumped parameter simulation model to include multiple thermal junctions.
    - The model simplification approach based on reduced order models and the definition of symmetry BCs.

- The evaluation of the thermal characteristics of alabandite based on experimental and simulation procedures.

4. **CAE implementation:**
   - A SAMCEF-ANSYS original implementation was completed for the standalone heat source lumped parameter model.
   - A SAMCEF-Patran original implementation was completed for the multi-chip lumped parameter model.
   - A SAMCEF-Patran original implementation was completed for developing the FEM PID controller.
   - An ANSYS Mechanical original implementations was completed for evaluating the thermal characteristics of alabandite
   - An ANSYS Fluent original implementation was completed for deciding the optimal configuration of the bonded heat sink.
5. **Experimental procedure**:
   - The development of new temperature acquisition procedures and processing of the results.

Future work will focus on the following objectives:

1. **The development of an algorithm for minimizing the temperature acquisition error when the heat sources operate at low power:** the accuracy of the lumped parameter model relies on the resolution of the acquisition system. In this regard, conventional temperature sensors are not able to capture the thermal gradients that occur in the first operational states of the instruction cycle. From this perspective, a feedback procedure can be developed to minimize the acquisition noise and enhance the accuracy of the experimental data. In this way, the fidelity of the lumped parameter model can be improved without employing expensive experimental devices.
2. **Extending the generalization abilities of the ML regression algorithm:** to this end, the neural models depicted in Chapter 3 have the ability to generalize the thermal behaviour of heat sources that belong to the same family. Features such as packaging technology, soldering technique or geometric characteristics can be considered in the dataset development process. In this way, the temperature gain and time constants can be predicted for a broader range of electronic components.
3. **Including all the derived experimental knowledge in a database for future use:** the time constants and temperature gains employed for parameterizing the lumped parameter model represent a valuable source of engineering knowledge. In this regard, a database can be developed to facilitate the future use of the experimental data.
4. **The expansion of the FEM PID temperature control methodology to include a model-based tuning procedure:** the Zielger-Nichols heuristic method employed for tuning the controller demands carrying out an iterative approach for deriving the initial gains. From this perspective, a model-based procedure can prove less time consuming while providing better performance characteristics. Such tuning algorithms can be included in the programming environment of the FEM solver.
5. **Investigating the use of nanopowders for coating the external walls of alabandite fins:** the acrylic primer enriched with graphite powder helps prevent manganese oxidation. Even so, this coating technology does not influence the thermal characteristics of alabandite. From this perspective, the use of nanopowders (i.e. copper or aluminium nanoparticles) can

significantly improve the heat transfer abilities of alabandite fins. Thus, future work is needed for developing a bonding agent that can facilitate the adhesion between nanopowders and manganese oxide.

6. **The analysis of multiple bonded heat sink configurations for facilitating the use of fins manufactured from alternative materials:** the bonded heat sink design proposed in Chapter 5 represents one of the many options available. In this regard, various cold plate shapes can be employed for enhancing the thermal resistance characteristics while facilitating the more effective use of alabandite in cooling systems.
7. **The study of multiple types of tailing for heat sink design purposes:** in Romania, tailing dumps represent a significant environmental concern. Large quantities of solid waste can be found in the Apuseni Mountains, Baia Mare and the Moldovian-Muntenian Carpathians regions. Example of materials include: pyrites, quartz, galena and sphalerite. The approach depicted in Chapter 5 can be employed for studying the feasibility of including such minerals in the thermal design process.
8. **Integrating all the given concepts into a graphical user interface:** the effective capture and re-use of engineering knowledge can be carried out by developing a single graphical user interface that encompasses the given concepts in a common framework. In this way, the embedded systems cooling workflow in Smart retrofitting can be tackled by means of wizards, guidelines and checklists.

References

[***01] *** (2007), Date statistice aferente energiei electrice produse în anul 2007, Autoritatea Nationala de Reglementare în domeniul Energiei., Bucuresti

[***02] *** (2018), ANSYS 19.0 User's Manual, ANSYS Inc., Canonsburg

[***03] *** (2013), SAMCEF User's Manual, LMS Samtech, Liege

[A02] Abukhalil, T., Almahafzah, H., Alksasbeh, M., & Alqaralleh, B. A. (2020). Power optimization in mobile robots using a real-time heuristic. Journal of Robotics, 2020.

[A05] Ahmed, S., Kim, S., & Wallace, K. M. (2007). A methodology for creating ontologies for engineering design.

[A06] Al-Doori, W. H. A. R. (2011). Enhancement of natural convection heat transfer from the rectangular fins by circular perforations. International journal of automotive and mechanical engineering, 4, 428-436.

[A07] Alexandru, T. G., & Pupaza, C. (2017). Eco-design of heat sinks based on CAD/CAE techniques. Proceedings in Manufacturing Systems, 12(1), 9.

[A09] Alexandru, T. G., & Pupăză, C. (2020). Machine learning generalization of lumped parameter models for the optimal cooling of embedded systems. Studies in Informatics and Control, 29(2), 169-177.

[A10] Alexandru, T. G., Mantea, T. A., Pupaza, C., & Velicu, S. (2016). Heat transfer simulation for thermal management of electronic components. Proceedings in Manufacturing Systems, 11(1), 15.

[A11] Alexandru, T.G. (2019, September). CISA Seminar - An approach for facilitating thermal design through the use of intelligent systems for Industry 4.0. Available at: https://www.edinburgh-robotics.org/events/cisa-seminar-approach-facilitating-thermal-design-through-use-intelligent-systems-industry-40, accessed: 25.09.2021

[A12] Alexandru, T.G., & Pupăză, C. (2021). Reccurent neural network for predicting time step bisections in structural dynamics, 83(1), pp.169-180

[A13] Al-Maeeni, S. S. H., Kuhnhen, C., Engel, B., & Schiller, M. (2020). Smart retrofitting of machine tools in the context of industry 4.0. Procedia CIRP, 88, 369-374.

[A14] Ravi, D., Honnavalli, P.B. & Vijay, C.N. (2020, December). A System to Retrofit Existing Infrastructure to ve Smart and IoT Ready. In Proceedings of the 2020 4th International Conveference of Vision, Image and Signal Processing (pp. 1-6).

[A15] Amrouch, H., Ebi, T., Schneider, J., Parameswaran, S., & Henkel, J. (2013, September). Analyzing the thermal hotspots in FPGA-based embedded systems. In 2013 23rd International Conference on Field programmable Logic and Applications (pp. 1-4). IEEE.

[A16] Andrews, J. A. (1988). Package thermal resistance model: Dependency on equipment design. IEEE transactions on components, hybrids, and manufacturing technology, 11(4), 528-537.

[A17] Aneja, B., Singh, S., Chandna, U., & Maheshwari, V. (2011). Review of temperature measurement and control. Intl. Journal of Electrical and Electronics Engineers, 3(2), 29-37.

[A19] Arularasan, R., Dhanushkodi, G., & Velraj, R. (2011). CFD simulation studies and experimental validation on a parallel plate heat sink. International Journal of Computer Aided Engineering and Technology, 3(5-6), 526-537.

[A20] Aström, K. J., & Hägglund, T. (2004). Revisiting the Ziegler–Nichols step response method for PID control, Journal of process control, 14(6), pp.635-650.

[B01] Bahrami, M. (2014). Steady conduction heat transfer. Journal of King Saud University-Engineering Sciences, 135-224.

[B02] Bailey, D. H., Plouffe, S. M., Borwein, P. B., & Borwein, J. M. (1997) The quest for pi, The Mathematical Intelligencer, 19, pp.50-56

[B04] Bashar, A. (2019). Survey on evolving deep learning neural network architectures. Journal of Artificial Intelligence, 1(02), 73-82.

[B05] Bathe, K. J., & Khoshgoftaar, M. R. (1979). Finite element formulation and solution of nonlinear heat transfer. Nuclear Engineering and Design, 51(3), 389-401.

[B07] Bi, Q., Cai, W. J., Lee, E. L., Wang, Q. G., Hang, C. C., & Zhang, Y. (1999). Robust identification of first-order plus dead-time model from step response. Control Engineering Practice, 7(1), 71-77.

[B10] Bongomin, O., Yemane, A., Kembabazi, B., Malanda, C., Chikonkolo Mwape, M., Sheron Mpofu, N., & Tigalana, D. (2020). Industry 4.0 Disruption and Its Neologisms in Major Industrial Sectors: A State of the Art. Journal of Engineering, 2020.

[C01] Chen, Y., Dai, X., Liu, M., Chen, D., Yuan, L., & Liu, Z. (2020, August). Dynamic relu. In European Conference on Computer Vision (pp. 351-367). Springer, Cham.

[C02] Chen, Y., Han, Z., Cao, K., Zheng, X., & Xu, X. (2020). Manufacturing upgrading in industry 4.0 era. Systems Research and Behavioral Science, 37(4), 766-771.

[C04] Coelho, T.M., Nogueira, E.S., Pereira, J.R.D., Baesso, M. L., & Bento, A.C. (2005). Thermal properties of thin acrylic paints using thermal wave interferometry, Journal de Physique IV (Proceedings), 125, pp. 519-522.

[C05] Contreras, J. D., Garcia, J. I., & Pastrana, J. D. (2017). Developing of Industry 4.0 Applications. International Journal of Online Engineering, 13(10).

[D01] da Silva, L. R., Flesch, R. C. C., & Normey-Rico, J. E. (2020). Controlling industrial dead-time systems: When to use a PID or an advanced controller. ISA transactions, 99, 339-350.

[D02] Dalenogare, L. S., Benitez, G. B., Ayala, N. F., & Frank, A. G. (2018). The expected contribution of Industry 4.0 technologies for industrial performance. International Journal of Production Economics, 204, 383-394.

[D03] Das, A. P., Sukla, L. B., Pradhan, N., & Nayak, S. (2011). Manganese biomining: a review. Bioresource Technology, 102(16), 7381-7387.

[D04] De Micco, L., Vargas, F. L., & Fierens, P. I. (2019). A literature review on embedded systems. IEEE Latin America Transactions, 18(02), 188-205.

[D05] Dick, R. P., Lakshminarayana, G., Raghunathan, A., & Jha, N. K. (2003). Analysis of power dissipation in embedded systems using real-time operating systems. IEEE transactions on computer-aided design of integrated circuits and systems, 22(5), 615-627.

[D06] Dietrich, A., van de Sand, R., & Reiff-Stephan, J. (2021). Implementation of a machine tool retrofit system. TH Wildau Engineering and Natural Sciences Proceedings, 1.

[D07] Dinca, G. (2019), Mineralogia zacamântului de au-ag-te sacarâmb, cu privire speciala asupra sulfosarurilor, Doctoral Thesis, Universitatea din Bucuresti

[D08] Ding, S., Li, H., Su, C., Yu, J., & Jin, F. (2013). Evolutionary artificial neural networks: a review. Artificial Intelligence Review, 39(3), 251-260.

[D10] Dziurdzia, P., & Kos, A. (2000, March). High efficiency active cooling system. In Sixteenth Annual IEEE Semiconductor Thermal Measurement and Management Symposium (Cat. No. 00CH37068) (pp. 19-26). IEEE.

[E01] Edalatifar, M., Tavakoli, M. B., Ghalambaz, M., & Setoudeh, F. (2020). Using deep learning to learn physics of conduction heat transfer. Journal of Thermal Analysis and Calorimetry, 1-18.

[E02] EKL-Ag (2020), Heat sinks for industrial applications, Available at: https://www.ekl-ag.de/en/products/heatsinks-industry, accessed: 25.09.2021

[F01] Faulkner, D., Khotan, M., & Shekarriz, R. (2004). Managing electronics thermal management. Heat Transfer Engineering, 25(2), 1-4.

[G01] García, J. I., Cano, R. E., & Contreras, J. D. (2020). Digital retrofit: A first step toward the adoption of Industry 4.0 to the manufacturing systems of small and medium-sized enterprises. Proceedings of the Institution of Mechanical Engineers, Part B: Journal of Engineering Manufacture, 234(8), 1156-1169.

[G02] Garimella, S. V., Fleischer, A. S., Murthy, J. Y., Keshavarzi, A., Prasher, R., Patel, C., ... & Raad, P. E. (2008). Thermal challenges in next-generation electronic systems. IEEE Transactions on Components and Packaging Technologies, 31(4), 801-815.

[G03] Gevrey, M., Dimopoulos, I., & Lek, S. (2003). Review and comparison of methods to study the contribution of variables in artificial neural network models. Ecological modelling, 160(3), 249-264.

[G04] Górecki, K., Zarębski, J., Górecki, P., & Ptak, P. (2019). Compact thermal models of semiconductor devices–a review. International Journal of Electronics and Telecommunications, 65(2), 151-158.

[G06] Grimes, S., Donaldson, J., & Gomez, G. C.. (2014) Report on the environmental benefits of recycling, Bureau of International Recycling, London

[G07] Grujicic, M., Zhao, C. L., & Dusel, E. C. (2005). The effect of thermal contact resistance on heat management in the electronic packaging. Applied Surface Science, 246(1-3), 290-302.

[G08] Guerreiro, B. V., Lins, R. G., Sun, J., & Schmitt, R. (2018). Definition of Smart Retrofitting: First steps for a company to deploy aspects of Industry 4.0. In Advances in Manufacturing (pp. 161-170). Springer, Cham.

[G09] Guyer, E. C. (1999). Handbook of applied thermal design. CRC press.

[H01] Hannemann, R. J. (2003). Thermal control of electronics: Perspectives and prospects.
[H03] Hefner, A. R., & Blackburn, D. L. (1994). Thermal component models for electrothermal network simulation. IEEE Transactions on Components, Packaging, and Manufacturing Technology: Part A, 17(3), 413-424.
[H04] Huang, H. C., & Usmani, A. S. (2012). Finite element analysis for heat transfer: theory and software. Springer Science & Business Media.
[I02] Intel Corporation (2001). Intel®Pentium® III Processor Thermal Design Guide
[I03] Irani, S., Shukla, S., & Gupta, R. (2003). Online strategies for dynamic power management in systems with multiple power-saving states. ACM Transactions on Embedded Computing Systems (TECS), 2(3), 325-346.
[I04] Isakov, E. (2004), Engineering formulas for metalcutting: presented in customary US and metric units of measure, Industrial Press Inc., New York
[J01] Jamal, R., Singh, I. K., Kumar, V., Chandel, A., & Singh, R. K. Introduction to Multiphysics Simulation for Integrated PCB Design and Operational Environment Analysis of Via.
[J02] Jenkins, T. (2005). A brief history of... semiconductors. Physics education, 40(5), 430.
[J03] Joseph, E. A., & Olaiya, O. O. (2017). Cohen-coon PID Tuning Method; A Better Option to Ziegler Nichols-PID Tuning Method. Enginerring Research, 2(11), 141-145.
[K01] Kamble, L. V., Pangavhane, D. R., & Singh, T. P. (2014). Heat transfer studies using artificial neural network-a review. International Energy Journal, 14(1).
[K02] Karlsson, R., & Luttropp, C. (2006). EcoDesign: what's happening? An overview of the subject area of EcoDesign and of the papers in this special issue. Journal of cleaner production, 14(15-16), 1291-1298.
[K04] Kheirkhahan, P. (2017, October). Robust anti-windup control design for pid controllers. In 2017 17th International Conference on Control, Automation and Systems (ICCAS) (pp. 1622-1627). IEEE.
[K05] Koçak, Y., & Şiray, G. Ü. (2021). New activation functions for single layer feedforward neural network. Expert Systems with Applications, 164, 113977.
[K08] Kumar, S., & Negi, R. (2012, December). A comparative study of PID tuning methods using anti-windup controller. In 2012 2nd International Conference on Power, Control and Embedded Systems (pp. 1-4). IEEE.
[L01] Lafon, F., Ramanujan, A., & Fernandez-Lopez, P. (2015). Black Box Model of Integrated Circuits for ESD Behavioral Simulation and Industrial Application Case. Advanced Electromagnetics, 4(2), 26-37.
[L04] Langley, P., & Simon, H. A. (1995). Applications of machine learning and rule induction. Communications of the ACM, 38(11), 54-64.
[L05] Lasance, C., Vinke, H., Rosten, H., & Weiner, K. L. (1995, February). A novel approach for the thermal characterization of electronic parts. In Proceedings of 1995 IEEE/CPMT 11th Semiconductor Thermal Measurement and Management Symposium (SEMI-THERM) (pp. 1-9). IEEE.
[L06] Laudani, A., Lozito, G. M., Riganti Fulginei, F., & Salvini, A. (2015). On training efficiency and computational costs of a feed forward neural network: a review. Computational intelligence and neuroscience, 2015.
[L07] Lee, E. A., & Seshia, S. A. (2017). Introduction to embedded systems: A cyber-physical systems approach. Mit Press.
[L08] Lee, H. S. (2010). Thermal design: heat sinks, thermoelectrics, heat pipes, compact heat exchangers, and solar cells. John Wiley & Sons.
[L09] Lee, S. (1995). Optimum design and selection of heat sinks. IEEE Transactions on Components, Packaging, and Manufacturing Technology: Part A, 18(4), 812-817.
[L12] Li, Y., Carabelli, S., Fadda, E., Manerba, D., Tadei, R., & Terzo, O. (2020). Machine learning and optimization for production rescheduling in Industry 4.0. The International Journal of Advanced Manufacturing Technology, 110(9), 2445-2463
[L14] Lima, F., Massote, A. A., & Maia, R. F. (2019, October). IoT energy retrofit and the connection of legacy machines inside the Industry 4.0 concept. In IECON 2019-45th Annual Conference of the IEEE Industrial Electronics Society (Vol. 1, pp. 5499-5504). IEEE.
[L16] Lobur, M., Salo, Y., Farmaha, I., Senkovych, O., & Pytel, K. (2021, May). Automated ARM CPU-Based Cloud System for the Industrial Internet of Things. In 2021 IEEE XVII th International Conference on the Perspective Technologies and Methods in MEMS Design (MEMSTECH) (pp. 25-28). IEEE.

[M01] Mahesh, B. (2020). Machine Learning Algorithms-A Review. International Journal of Science and Research (IJSR).[Internet], 9, 381-386.
[M02] Mantea, T. A., Alexandru, T. G., Pupăză, C., & Nicolescu, A. F. (2016). Software Integration for Heat Transfer Simulation of Electronic Circuits. Studies in Informatics and Control, 25(1), 70.
[M03] Marilungo, E., Papetti, A., Germani, M., & Peruzzini, M. (2017). From PSS to CPS design: a real industrial use case toward Industry 4.0. Procedia Cirp, 64, 357-362.
[M04] Masood, T., & Sonntag, P. (2020). Industry 4.0: Adoption challenges and benefits for SMEs. Computers in Industry, 121, 103261.
[M05] Meng, X., Thörnberg, B., & Olsson, L. (2012, September). Component obsolescence management model for long life cycle embedded system. In 2012 IEEE AUTOTESTCON Proceedings (pp. 19-24). IEEE.
[M06] Mugisha, J. C., Munyazikwiye, B., & Karimi, H. R. (2015, November). Design of temperature control system using conventional PID and Intelligent Fuzzy Logic controller. In 2015 International Conference on Fuzzy Theory and Its Applications (iFUZZY) (pp. 50-55). IEEE.
[M07] Myers, R. H., & Myers, R. H. (1990). Classical and modern regression with applications (Vol. 2, p. 488). Belmont, CA: Duxbury press.
[M09] Narasimhan, S., & Majdalani, J. (2002). Characterization of compact heat sink models in natural convection. IEEE Transactions on Components and Packaging Technologies, 25(1), 78-86.
[M10] Naresh, G., Sai, G. A., Abhiram, G., Sandeep, K. S., Vardhan, G. A., & Krishna, K. B. Steady State Thermal Analysis on Heat Sinks by Varying Fin Configuration Using ANSYS.
[M11] Niemann, H., & Miklos, R. (2014, December). A simple method for estimation of parameters in first order systems. In Journal of Physics: Conference Series (Vol. 570, No. 1, p. 012001). IOP Publishing.
[M12] Nikolskiy, V., & Stegailov, V. (2016). Floating-point performance of ARM cores and their efficiency in classical molecular dynamics. In Journal of Physics: Conference Series (Vol. 681, No. 1, p. 012049). IOP Publishing.
[M13] Nouman, K., Asim, Z., & Qasim, K. (2018, May). Comprehensive Study on Performance of PID Controller and its Applications. In 2018 2nd IEEE Advanced Information Management, Communicates, Electronic and Automation Control Conference (IMCEC) (pp. 1574-1579). IEEE.
[O01] Ongsulee, P. (2017, November). Artificial intelligence, machine learning and deep learning. In 2017 15th International Conference on ICT and Knowledge Engineering (ICT&KE) (pp. 1-6). IEEE.
[P01] Padula, F., & Visioli, A. (2011). Tuning rules for optimal PID and fractional-order PID controllers. Journal of process control, 21(1), 69-81.
[P02] Pagani, S., Manoj, P. S., Jantsch, A., & Henkel, J. (2018). Machine learning for power, energy, and thermal management on multicore processors: A survey. IEEE Transactions on Computer-Aided Design of Integrated Circuits and Systems, 39(1), 101-116.
[P04] Park, J. S., Jung, Y. K., Butler, K. T., & Walsh, A. (2018). Quick-start guide for first-principles modelling of semiconductor interfaces. Journal of Physics: Energy, 1(1), 016001.
[P07] Patil, D. S., Chavan, S. M., & Oubagaranadin, J. U. K. (2016). A review of technologies for manganese removal from wastewaters. Journal of Environmental Chemical Engineering, 4(1), 468-487.
[P10] Pivoto, D. G., de Almeida, L. F., da Rosa Righi, R., Rodrigues, J. J., Lugli, A. B., & Alberti, A. M. (2021). Cyber-physical systems architectures for industrial internet of things applications in Industry 4.0: A literature review. Journal of Manufacturing Systems, 58, 176-192.
[P12] Pupază, C., & Parpală, R. C. (2011). Modelare și analiză structurală cu ANSYS workbench (Structural Modeling and Analysis using Ansys workbench), Politehnica Press.
[R01] Raciti, A., & Cristaldi, D. (2013, October). Thermal modeling of integrated power electronic modules by a lumped-parameter circuit approach. In AEIT Annual Conference 2013 (pp. 1-6). IEEE.
[R03] Rejikumar, G., Arunprasad, P., Persis, J., & Sreeraj, K. M. (2019). Industry 4.0: key findings and analysis from the literature arena. Benchmarking: An International Journal.
[R05] Romeo, L., Loncarski, J., Paolanti, M., Bocchini, G., Mancini, A., & Frontoni, E. (2020). Machine learning-based design support system for the prediction of heterogeneous machine parameters in industry 4.0. Expert Systems with Applications, 140, 112869.
[R06] Ruder, S. (2016). An overview of gradient descent optimization algorithms. arXiv preprint arXiv:1609.04747.

[S01] Sabbah, W., Arabi, F., Avino-Salvado, O., Buttay, C., Théolier, L., & Morel, H. (2017). Lifetime of power electronics interconnections in accelerated test conditions: High temperature storage and thermal cycling. Microelectronics Reliability, 76, 444-449.

[S02] Sacala, I. S., Moisescu, M. A., & Repta, D. (2013, May). Towards the development of the future internet based enterprise in the context of cyber-physical systems. In 2013 19th International Conference on Control Systems and Computer Science (pp. 405-412). IEEE.

[S03] Saseendran, A., Setia, L., Chhabria, V., Chakraborty, D., & Barman Roy, A. (2019). Impact of Noise in Dataset on Machine Learning Algorithms.

[S04] Sasidhar, N., & Suresh, M. P. ARM microcontroller based Wireless Industrial Automation System. International Journal of Advanced Research in Electrical, Electronics and Instrumentation Engineering (IJAREEIE), 3.

[S06] Sazli, M. H. (2006). A brief review of feed-forward neural networks. Communications Faculty of Sciences University of Ankara Series A2-A3 Physical Sciences and Engineering, 50(01).

[S07] Schelling, P. K., Shi, L., & Goodson, K. E. (2005). Managing heat for electronics. Materials Today, 8(6), 30-35.

[S08] Schlechtendahl, J., Keinert, M., Kretschmer, F., Lechler, A., & Verl, A. (2015). Making existing production systems Industry 4.0-ready. Production Engineering, 9(1), 143-148.

[S09] Schweitzer, D., Ender, F., Hantos, G., & Szabó, P. G. (2015). Thermal transient characterization of semiconductor devices with multiple heat sources—Fundamentals for a new thermal standard. Microelectronics Journal, 46(2), 174-182.

[S10] Seidman, T. I. (1988, December). Some problems with thermostat nonlinearities. In Proc. 27th IEEE Conf. Decision and Control (pp. 1255-1259).

[S11] Sen, M. (2004). A review of principles and applications of thermal control. Ingeniería Mecánica. Tecnología y Desarrollo, 1(4), 115-131.

[S12] Sezer, E., Romero, D., Guedea, F., Macchi, M., & Emmanouilidis, C. (2018, June). An industry 4.0-enabled low cost predictive maintenance approach for smes. In 2018 IEEE International Conference on Engineering, Technology and Innovation (ICE/ITMC) (pp. 1-8). IEEE.

[S13] Shapiro, B. (2003). Creating compact models of complex electronic systems: An overview and suggested use of existing model reduction and experimental system identification tools. IEEE Transactions on Components and Packaging Technologies, 26(1), 165-172.

[S14] Shenkman, A. L. (2006). Transient analysis of electric power circuits handbook. Springer Science & Business Media.

[S15] Shinohara, A. C., da Silva, E. H. D. R., de Lima, E. P., Deschamps, F., & da Costa, S. E. G. (2017). Critical success factors for digital manufacturing implementation in the context of industry 4.0. In IIE Annual Conference. Proceedings (pp. 199-204). Institute of Industrial and Systems Engineers (IISE).

[S16] Simoncelli, E., & Daw, N. (2003). Least squares optimization. Lecture Notes, Available at: http://www.cns.nyu.edu/eero/teaching.html, accessed: 25.09.2021

[S18] Singh, K. K., & Agnihotri, G. (2012). System Design Through Matlab®, Control Toolbox and Simulink®. Springer Science & Business Media.

[S19] Singhala, P., Shah, D., & Patel, B. (2014). Temperature control using fuzzy logic. arXiv preprint arXiv:1402.3654.

[S20] Smolinski, P., & Wu, Y. S. (1998). An implicit multi-time step integration method for structural dynamics problems. Computational Mechanics, 22(4), 337-343.

[T01] Terol, R. M., Reina, A. R., Ziaei, S., & Gil, D. (2020). A Machine Learning Approach to Reduce Dimensional Space in Large Datasets. IEEE Access, 8, 148181-148192.

[T03] Thompson, N. C., Greenewald, K., Lee, K., & Manso, G. F. (2020). The computational limits of deep learning. arXiv preprint arXiv:2007.05558.

[T04] Torrico, B. C., de Almeida Filho, M. P., Lima, T. A., Forte, M. D. D. N., Sá, R. C., & Nogueira, F. G. (2018). Tuning of a dead-time compensator focusing on industrial processes. ISA transactions, 83, 189-198.

[T05] Tsavnin, A., Efimov, S., & Zamyatin, S. (2020). Overshoot elimination for control systems with parametric uncertainty via a PID controller. Symmetry, 12(7), 1092.

[T06] Tudor, G. A., & Pupaza, C. (2021). The development of PID temperature controllers based on FEM thermal analysis. In MATEC Web of Conferences (Vol. 342). EDP Sciences.

[W01] Wan, J., Tang, S., Shu, Z., Li, D., Wang, S., Imran, M., & Vasilakos, A. V. (2016). Software-defined industrial internet of things in the context of industry 4.0. IEEE Sensors Journal, 16(20), 7373-7380.
[W03] Wang, W., & Yuan, X. (2016). Lumped-parameter-based thermal analysis for virtual prototyping of power electronics systems.
[W04] Wang, X., Castellazzi, A., & Zanchetta, P. (2013, September). Temperature control for reduced thermal cycling of power devices. In 2013 15th European Conference on Power Electronics and Applications (EPE) (pp. 1-10). IEEE.
[W06] Weisberg, S. (2005). Applied linear regression (Vol. 528). John Wiley & Sons.
[W07] Wilcox, R. R. (1996). Confidence intervals for the slope of a regression line when the error term has nonconstant variance. Computational Statistics & Data Analysis, 22(1), 89-98.
[W08] Wu, R., Wang, H., Pedersen, K. B., Ma, K., Ghimire, P., Iannuzzo, F., & Blaabjerg, F. (2016). A temperature-dependent thermal model of IGBT modules suitable for circuit-level simulations. IEEE Transactions on Industry Applications, 52(4), 3306-3314.
[Z01] Zakoldaev, D. A., Shukalov, A. V., Zharinov, I. O., & Zharinov, O. O. (2019, April). Organization of information exchange between digital companies of Industry 4.0. In IOP Conference Series: Materials Science and Engineering (Vol. 510, No. 1, p. 012021). IOP Publishing.
[Z02] Zhang, K., Guliani, A., Ogrenci-Memik, S., Memik, G., Yoshii, K., Sankaran, R., & Beckman, P. (2017). Machine learning-based temperature prediction for runtime thermal management across system components. IEEE Transactions on parallel and distributed systems, 29(2), 405-419.